



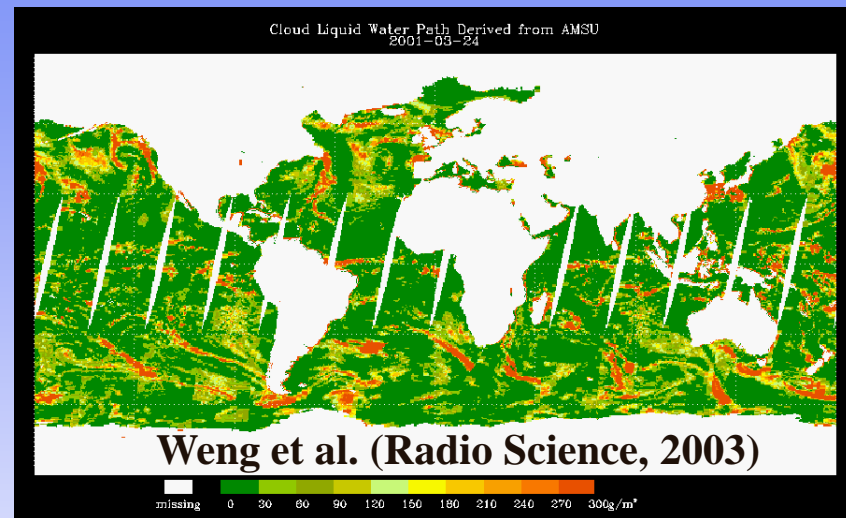
Microwave Integrated Retrieval “System” (MIRS)



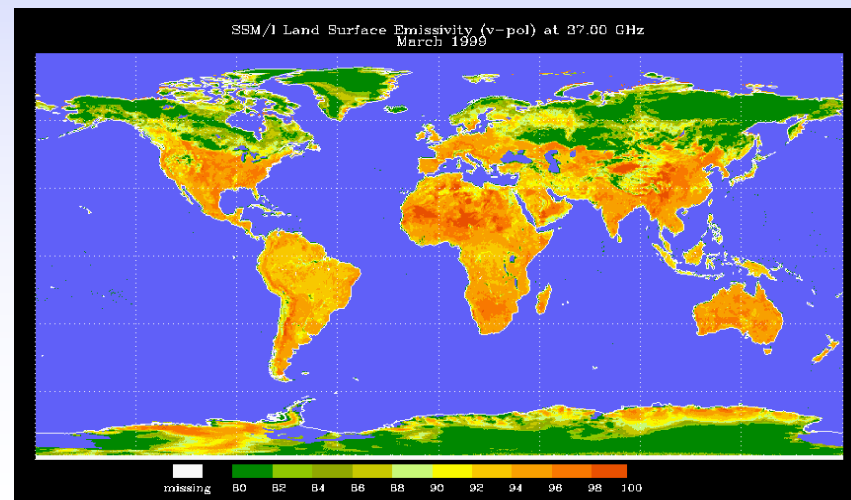
Objectives

- Enhance Microwave Surface and Precipitation Products System (MSPPS) Performance
- Provide front-end retrievals for the robust first guess to infrared sounding system (HIRS, hyperspectral)
- Profile temperature, water vapor and cloud water from microwave instrument under all weather conditions
- Improve profiling lower troposphere by using more “surface viewing” channels in retrieval algorithm
- Integrate the state-of-the-art radiative transfer model components from JCSDA into MIRS
- Prepare for future microwave sounding system (e.g. ATMS, CMIS, SSMIS, Geo-MW)

AMSU Cloud Liquid Water Path (3/24, 2001)



Microwave surface Emissivity at 37 GHz





ORA Microwave Remote Sensing Roadmap

2006 2007 2008 2009 2010 2011 2012 2013 2014 2015

Integrated calibration and validation system for
POES, NPP, NPOESS microwave sensors

Geostationary microwave sounder and imager concept,
requirements, risk reduction studies

Microwave integrated retrieval system for sounding and non-sounding products
from NPOESS CMIS and ATMS

Geo-MW calibration algorithms sciences and algorithms

Synergetic uses of GOES-R HES and MW for profiling under all weather
conditions

Inter-satellite calibrations using
NPOESS and GOES-R microwave
sensors

Uses of POES and NPOESS microwave data under all weather conditions
through using JCSDA community radiative transfer models including
scattering, polarimetry, surface emissivity models

Prepare for uses of GOES-R microwave data for severe
storm monitoring and prediction in Hurricane WRF
models through 4DDA

POES

GOES

Applications

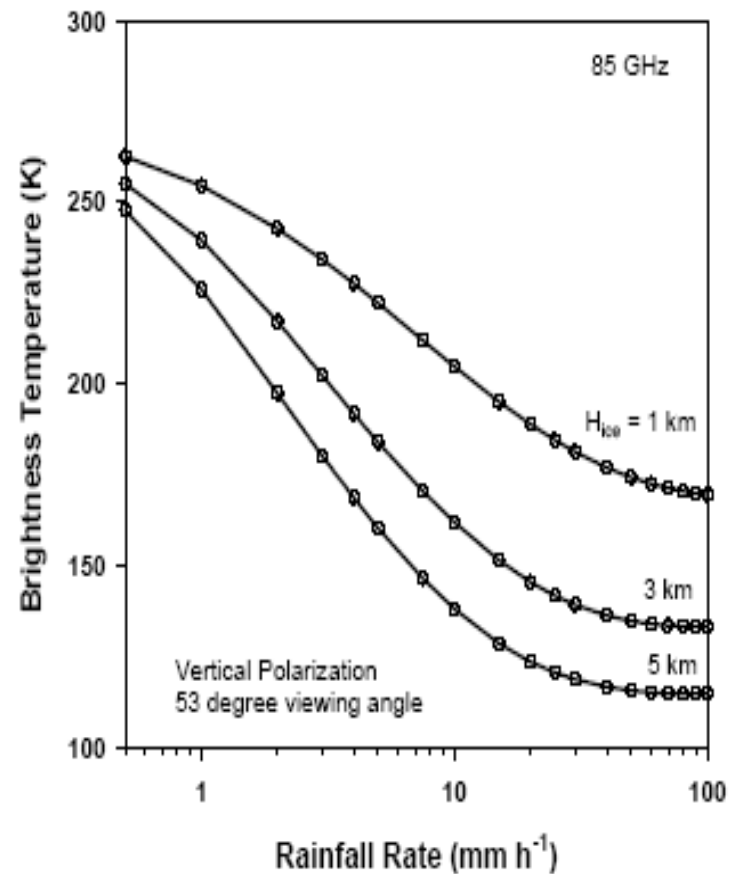
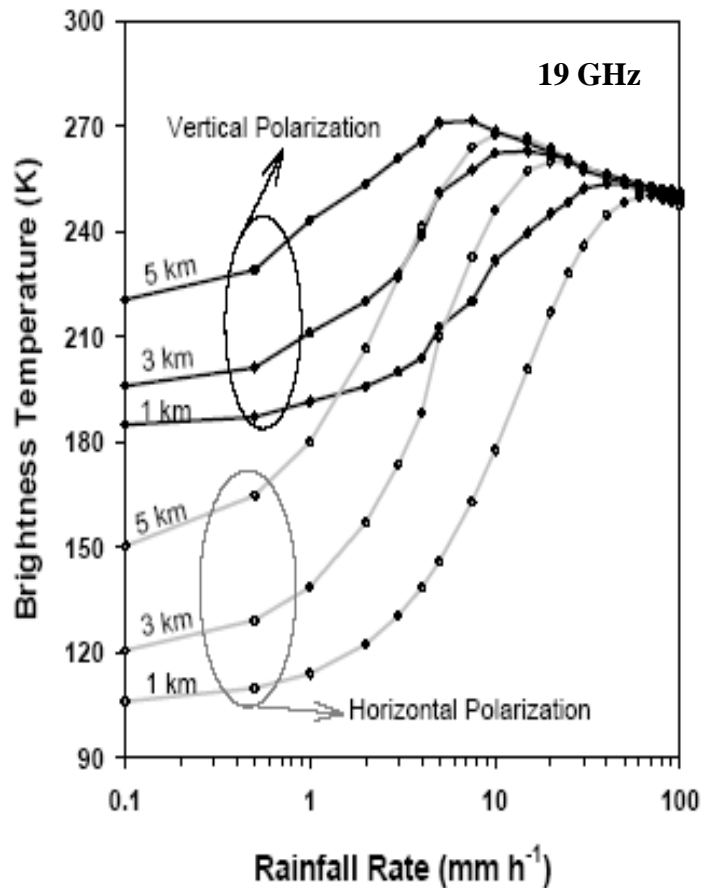


Microwave Products from NPOESS CMIS

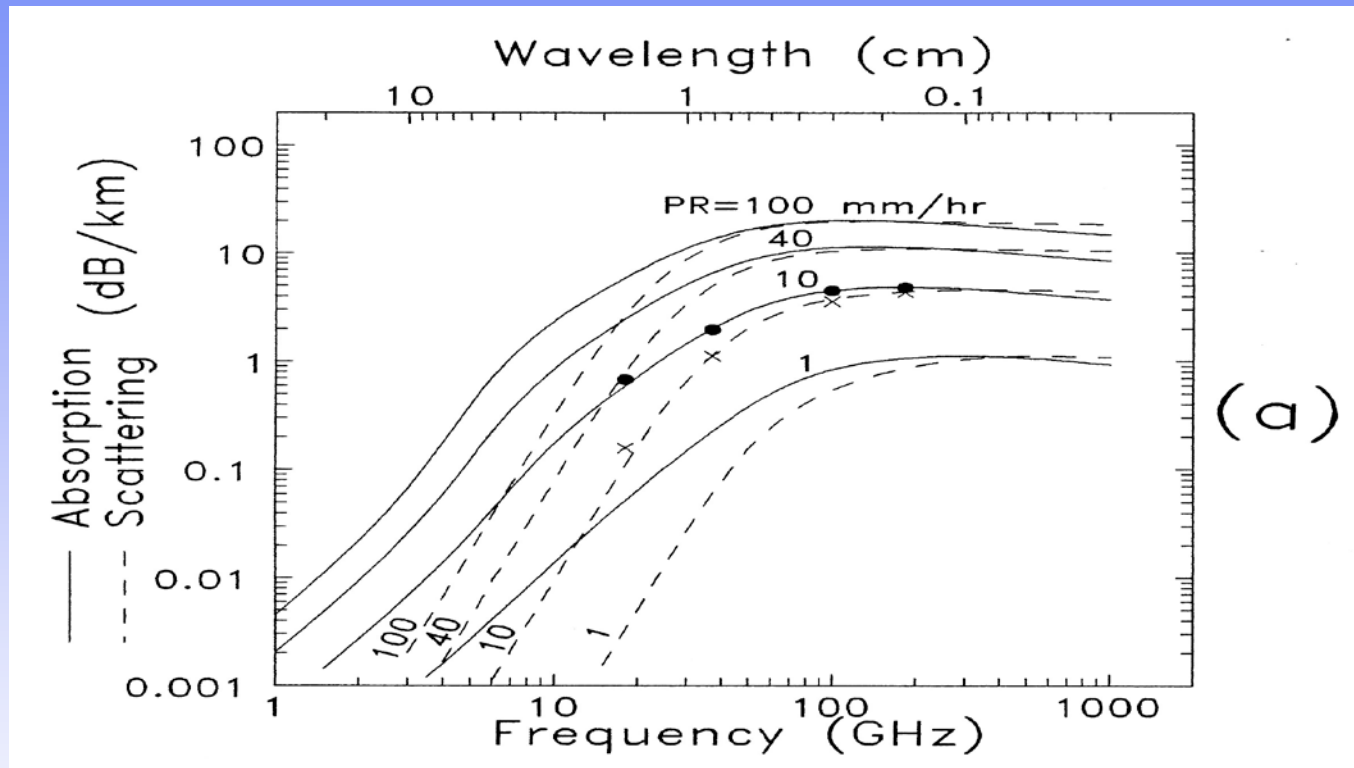
| EDR Title | Category |
|--|----------------|
| <i>Atmospheric Vertical Moisture Profile (surf to 600mb)</i> | <i>IA</i> |
| Sea Surface Winds (Speed) | IA |
| Soil Moisture | IA |
| <i>Atmospheric Vertical Moisture Profile (600 to 100mb)</i> | <i>IIA</i> |
| <i>Atmospheric Vertical Temperature Profile</i> | <i>IIA</i> |
| <i>Cloud Ice Water Path</i> | <i>IIA</i> |
| <i>Cloud Liquid Water</i> | <i>IIA</i> |
| Ice Surface Temperature | IIB |
| <i>Land Surface Temperature</i> | <i>IIB</i> |
| <i>Precipitation</i> | <i>IIA</i> |
| <i>Precipitable Water</i> | <i>IIA</i> |
| Sea Ice Age and Sea Ice Edge Motion | IIB |
| Sea Surface Temperature | IIA |
| Sea Surface Winds (Direction) | IIA |
| <i>Total Water Content</i> | <i>IIA</i> |
| Cloud Base Height | IIIB |
| Fresh Water Ice | IIIB |
| Imagery | IIIB |
| Pressure Profile | IIIB |
| <i>Snow Cover / Depth</i> | <i>III B/A</i> |
| Surface Wind Stress | IIIB |
| Vegetation / Surface Type | IIIB |

*The highlighted are
operational EDRS
derived from POES AMSU*

Effects of Clouds and Precipitation on Microwave Window Channels:



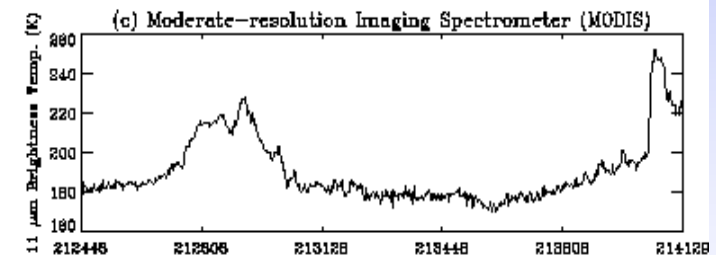
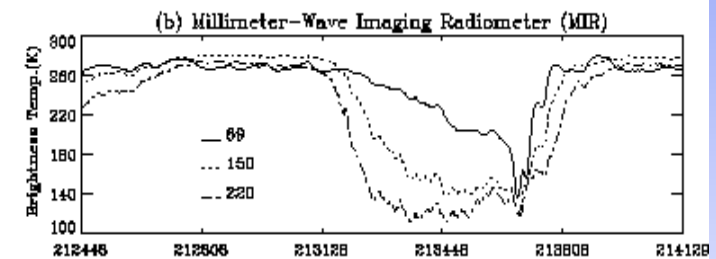
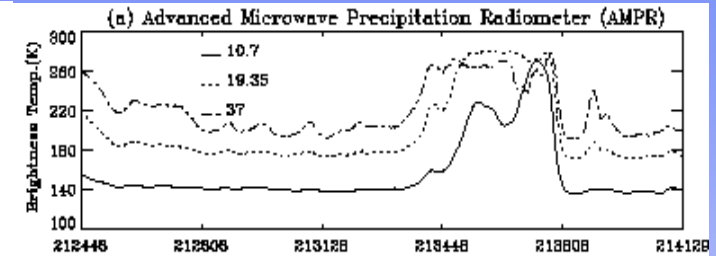
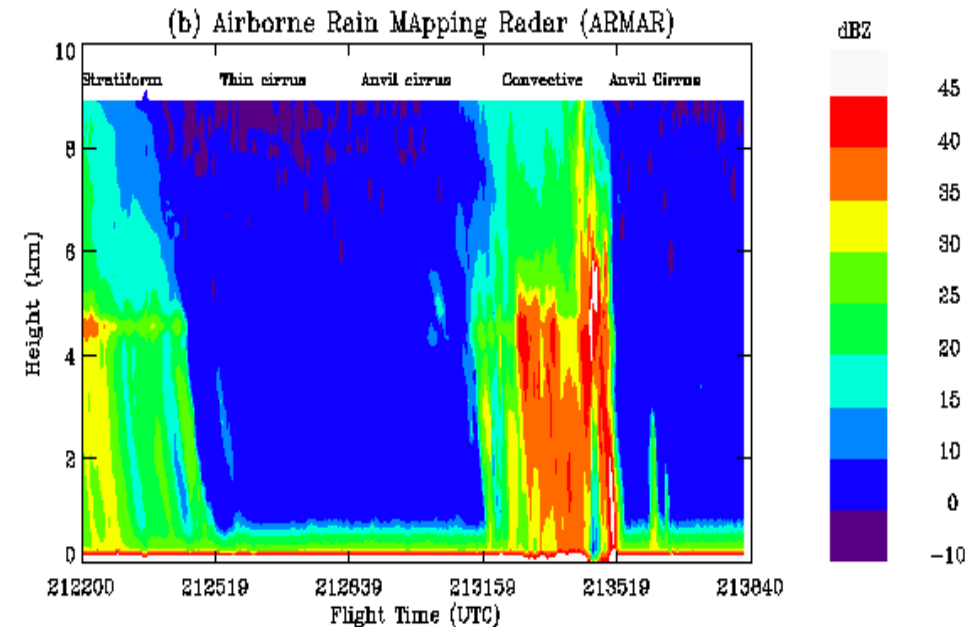
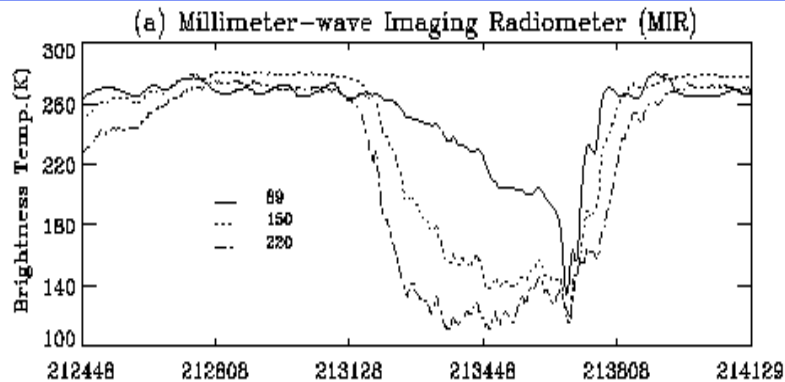
Cloud Absorption and Scattering



$$\sigma_{ext}(\lambda, z) \approx \sigma_{abs}(\lambda, z) \approx \frac{6\pi}{\lambda} \text{Im}(-K) \int_0^{\infty} \frac{4}{3} \pi r^3 n(r) dr = \frac{6\pi}{\lambda \rho_w} \text{Im}(-K) LWC(z)$$

$$\sigma_{sca}(\lambda, z) = \frac{128\pi^5}{3\lambda^4} |K|^2 \int_0^{\infty} r^6 n(r) dr = \frac{24\pi^3}{\lambda^4 \rho_i^2} |K|^2 \int_0^{\infty} n(r) M^2(r) dr$$

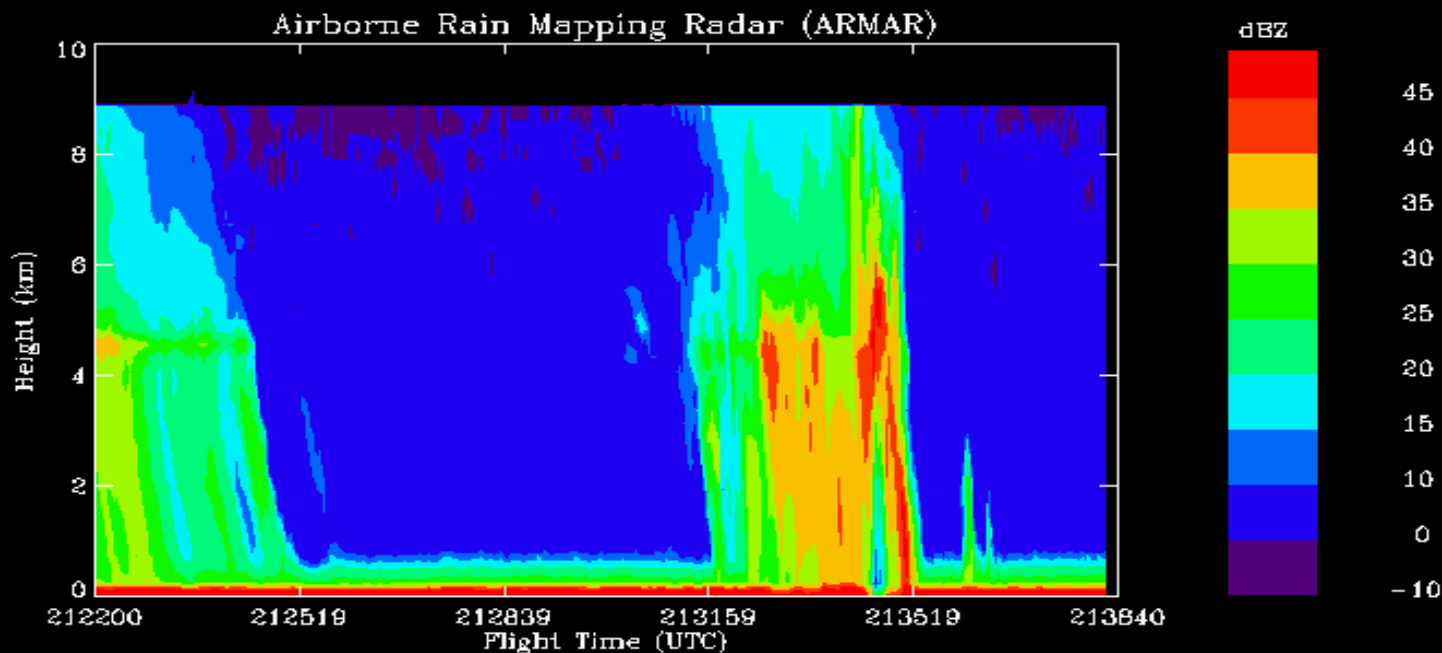
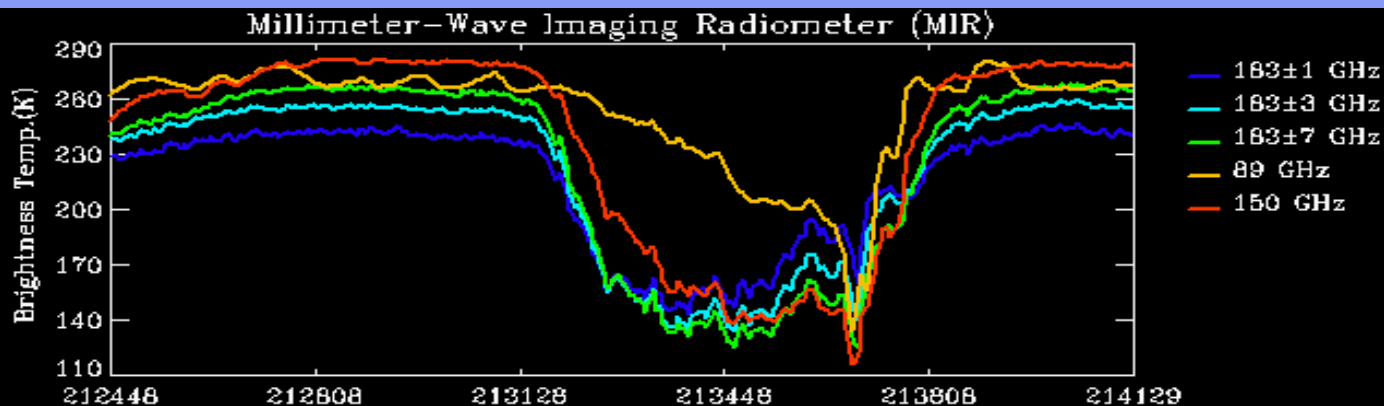
ER-2/DC-8 Measurements during TOGA/CORE (1/2)



Weng and Grody (2000, JAS)

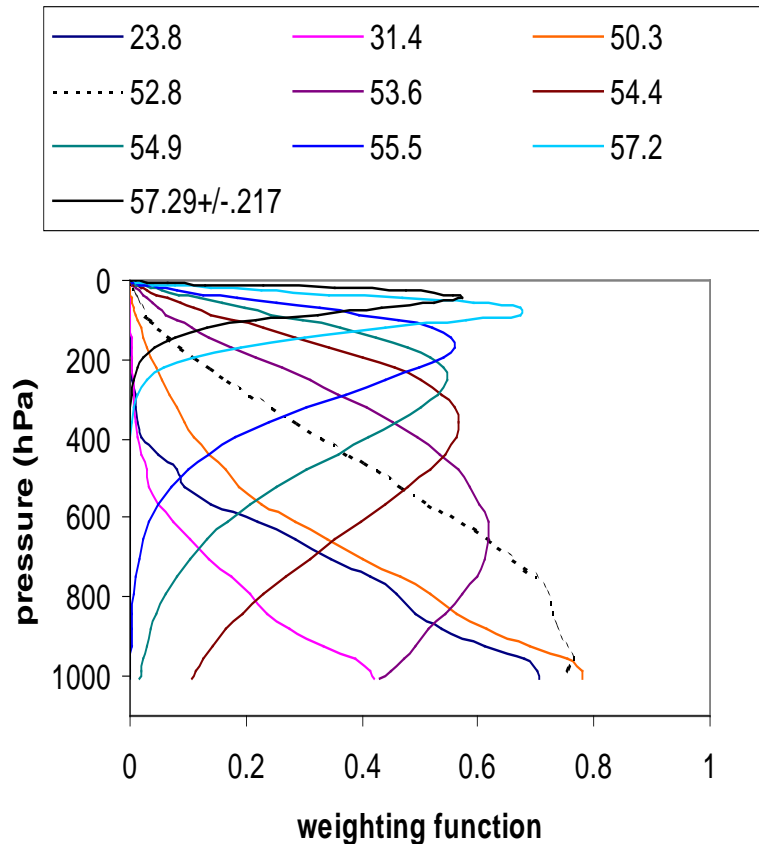


ER-2/DC-8 Measurements during TOGA/CORE (2/2)

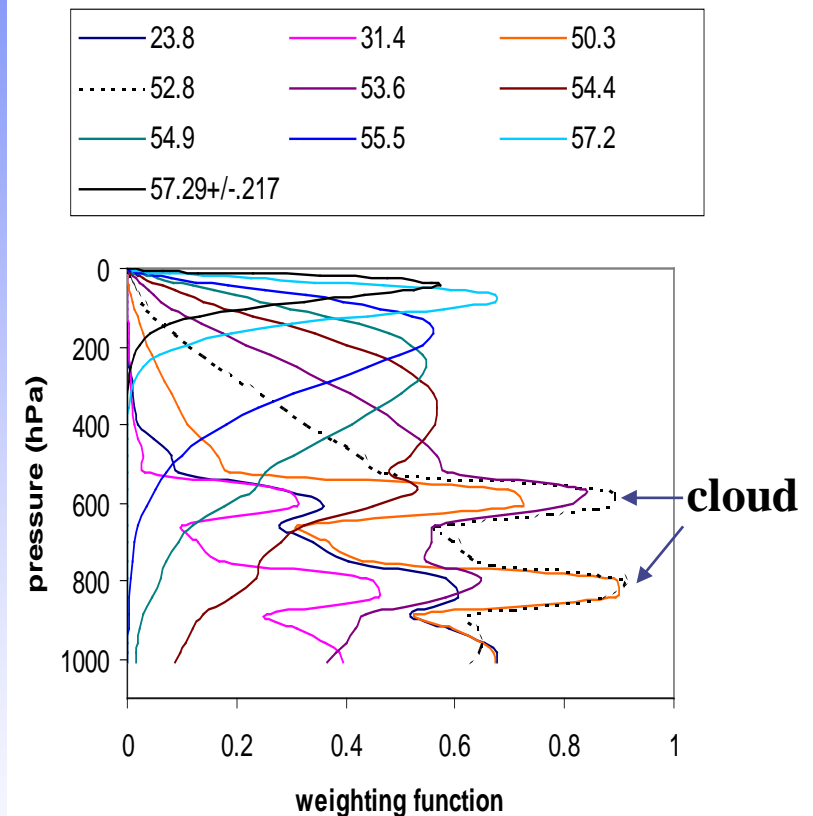




Clouds Modify AMSU Weighting Function



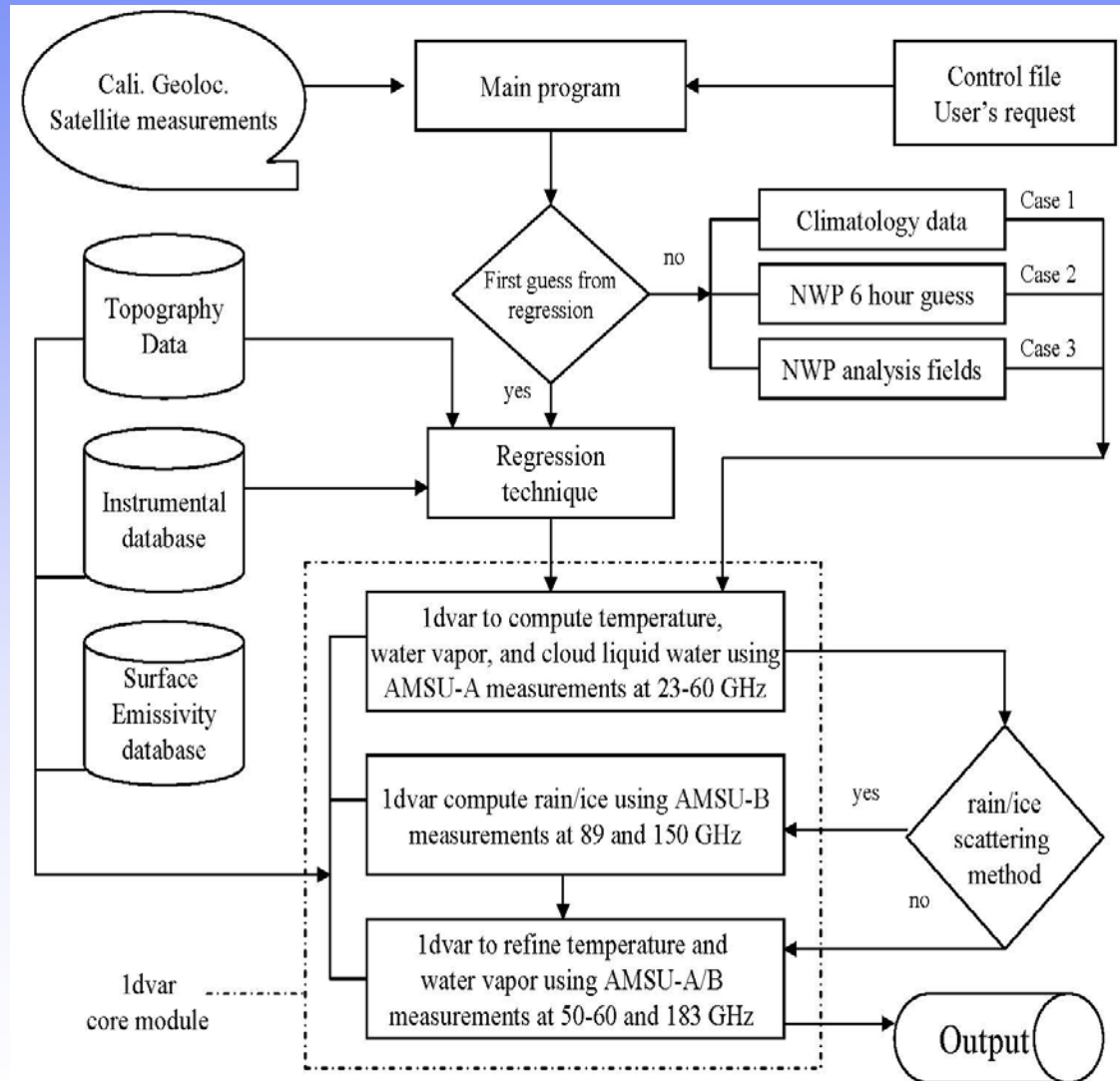
Clear condition



Include two separated cloud layers at
610 and 840 hPa with 0.5 g m^{-3} liquid water.

Microwave Integrated Retrieval System Flowchart

- Fast scattering/polarimetric radiative transfer model/Jacobian for all atmospheric conditions
- Surface emissivity/reflectivity models (soil, vegetation, snow/sea ice, water)
- Fast variational minimization algorithm
- NWP forecast outputs, climatology, regressions as first guess
- Temperature, water vapor and cloud and rain water profiles
- Flexible channel selection/sensor geometry and noise





Algorithm Theoretical Basis (1/9)

Cost Function:

$$J = \frac{1}{2} (\mathbf{x} - \mathbf{x}^b)^T \mathbf{B}^{-1} (\mathbf{x} - \mathbf{x}^b) + \frac{1}{2} [\mathbf{I}(\mathbf{x}) - \mathbf{I}^o]^T (\mathbf{E} + \mathbf{F})^{-1} [\mathbf{I}(\mathbf{x}) - \mathbf{I}^o]$$

where

\mathbf{x}_b is background vector

\mathbf{x} is state vector to be retrieved

\mathbf{I} is the radiance vector

\mathbf{B} is the error covariance matrix of background

\mathbf{E} is the observation error covariance matrix

\mathbf{F} is the radiative transfer model error matrix

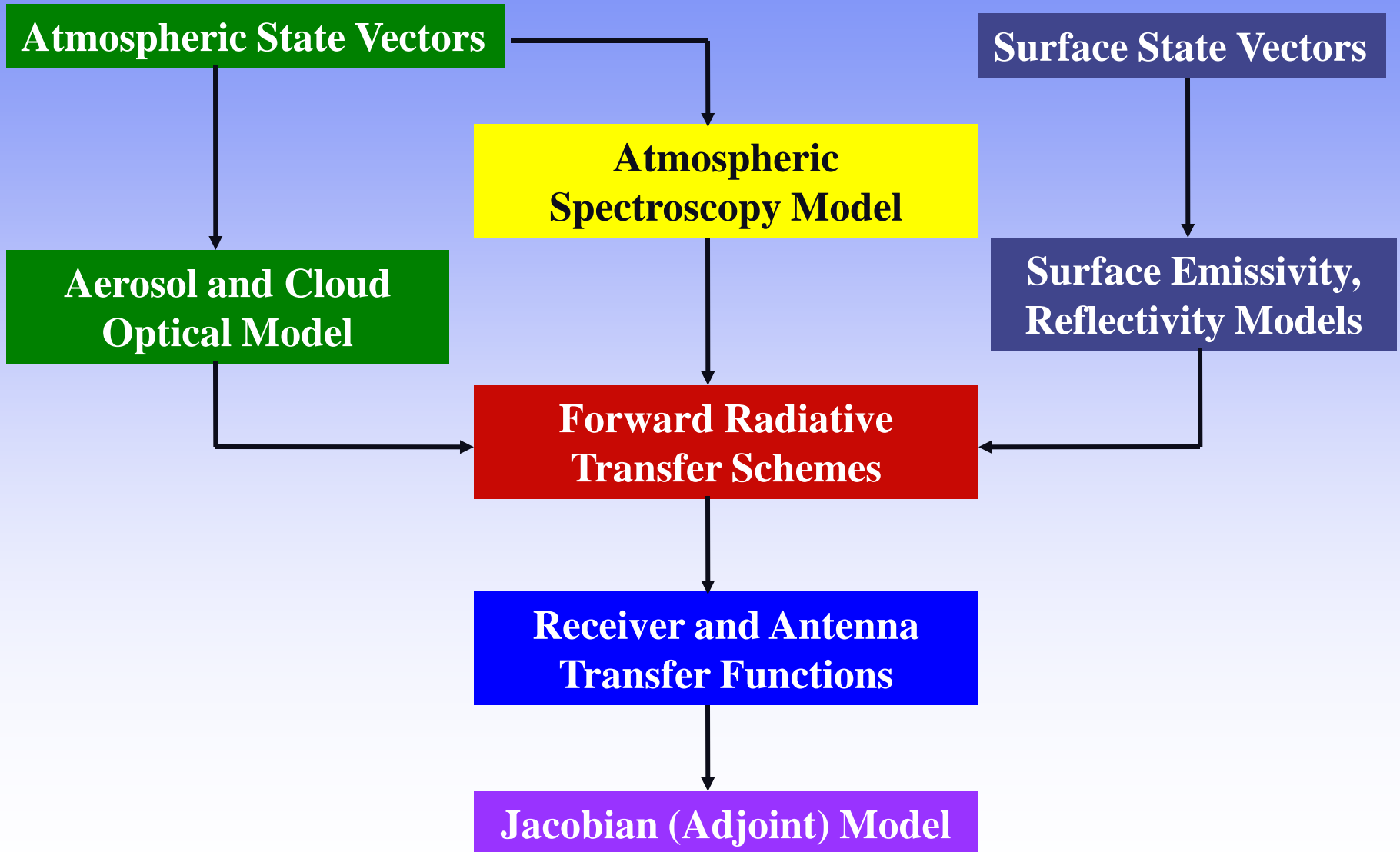


Algorithm Theoretical Basis (2/9)

- Retrievals are made at vertical pressure levels (0.1 to surface, maximum levels of 42)
- Surface pressure from GDAS 6-hour forecasts
- Background state variables from climatology which is latitude-dependent
- First guess is from regression (could be the same as background)
- No background information needed for cloud water
- Bias correction for forward models, residuals will be observational error covariance

Algorithm Theoretical Basis (3/9)

JCSDA Community Radiative Transfer Model





Algorithm Theoretical Basis (4/9)

Radiative Transfer Model:

$$\mu \frac{d\mathbf{I}(\tau, \Omega)}{d\tau} = -\mathbf{I}(\tau, \Omega) + \frac{\omega}{4\pi} \int_0^{4\pi} \mathbf{M}(\tau, \Omega, \Omega') \mathbf{I}(\tau, \Omega') d\Omega' + (1 - \omega) \mathbf{B} + \frac{\omega F_0}{4\pi} \exp(-\tau / \mu_0) \mathbf{S}$$

- Radiative transfer scheme including four Stokes components is based on VDISORT (Weng, JQRST, 1992)
- Accuracies on various transfer problems including molecular scattering, L13 aerosols and microwave polarimetry are discussed (Schulz et al., JQSRT, 1999, Weng, J. Elec&Appl., 2002)
- Jacobians including cloud liquid and ice water are derived using VDISORT solutions (Weng and Liu, JAS, 2003)
- Surface emissivity and bi-directional reflectivity models are integrated (Weng et al., JGR, 2001)

Algorithm Theoretical Basis (5/9)

Vector DIScrete Ordinate Radiative (VDISORT) Solution:

$$\mathbf{I}_l(\tau) = \exp[\mathbf{A}_l(\tau - \tau_{l-1})] \mathbf{c}_l + \mathbf{s}_l(\tau)$$

$$\begin{aligned} \mathbf{s}_l(\tau) = & \delta_{m0} [B(\tau_{l-1}) \mathbf{\Xi} + \frac{B(\tau_l) - B(\tau_{l-1})}{\tau_l - \tau_{l-1}} (\mathbf{A}_l^{-1} \mathbf{\Xi} + (\tau - \tau_{l-1}) \mathbf{\Xi})] \\ & + \mu_0 [\mu_0 \mathbf{A}_l + \mathbf{E}]^{-1} \frac{\omega F_0}{\pi} \exp(-\tau / \mu_0) \mathbf{\Psi} \end{aligned}$$

Jacobians Including Scattering:

$$\begin{aligned} \frac{\partial \mathbf{I}_1(\mu)}{\partial x_l} = & \sum_{k=l}^L \sum_{j=-4N}^{4N} \mathbf{K}_k(\mu, j) \left\{ \frac{\partial (\mathbf{s}_k(\tau) - \mathbf{s}_{k-1}(\tau))}{\partial x_l} \Big|_{\tau=\tau_{l-1}} \right\}_j + \delta_{1l} \frac{\partial \mathbf{s}_1(\mu)}{\partial x_l} \\ & - \sum_{j=-4N}^{4N} \mathbf{K}_l(\mu, j) \left\{ \frac{\partial}{\partial x_l} \exp[\mathbf{A}_l(\tau - \tau_{l-1})] \Big|_{\tau=\tau_l} \mathbf{c}_l \right\}_j \end{aligned}$$

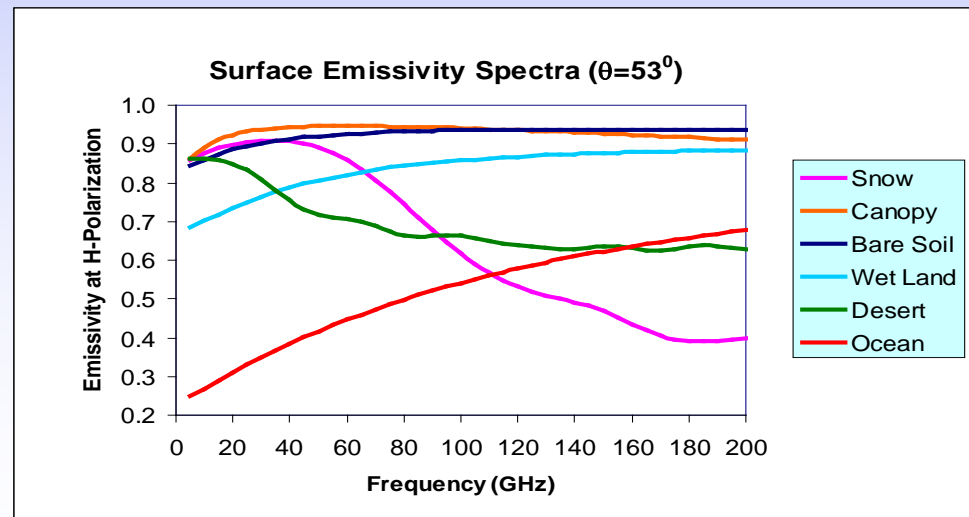
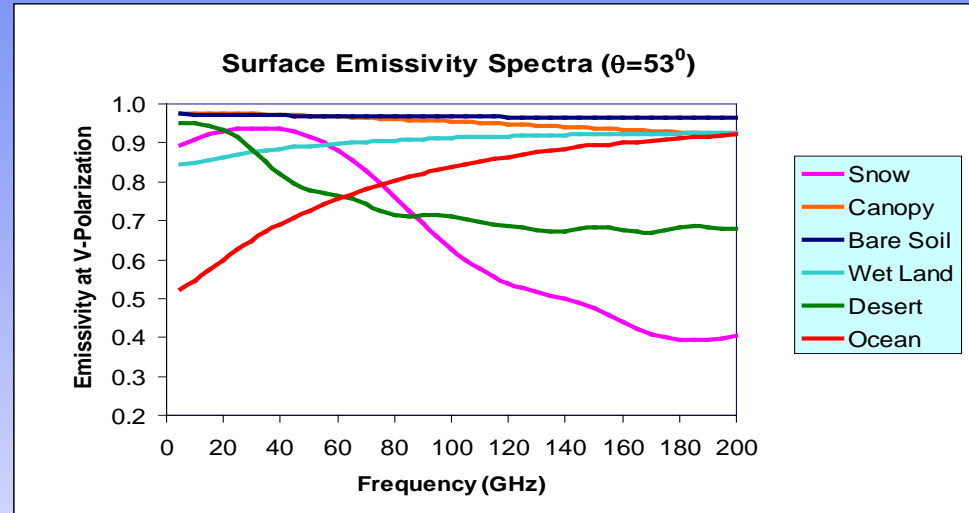
(Weng and Liu, JAS, 2003)

Algorithm Theoretical Basis (6/9)

Emissivity Model:

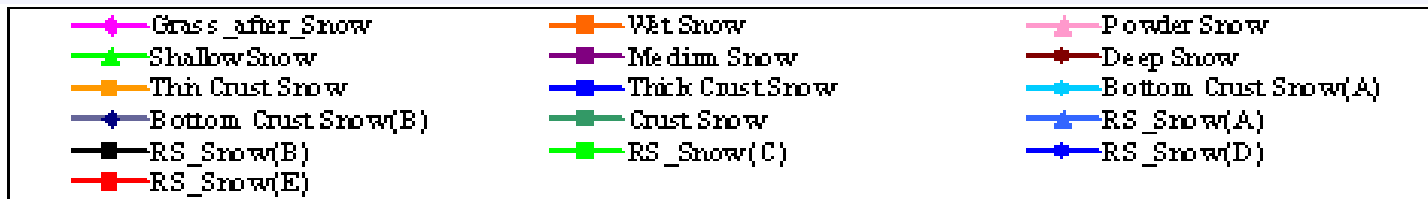
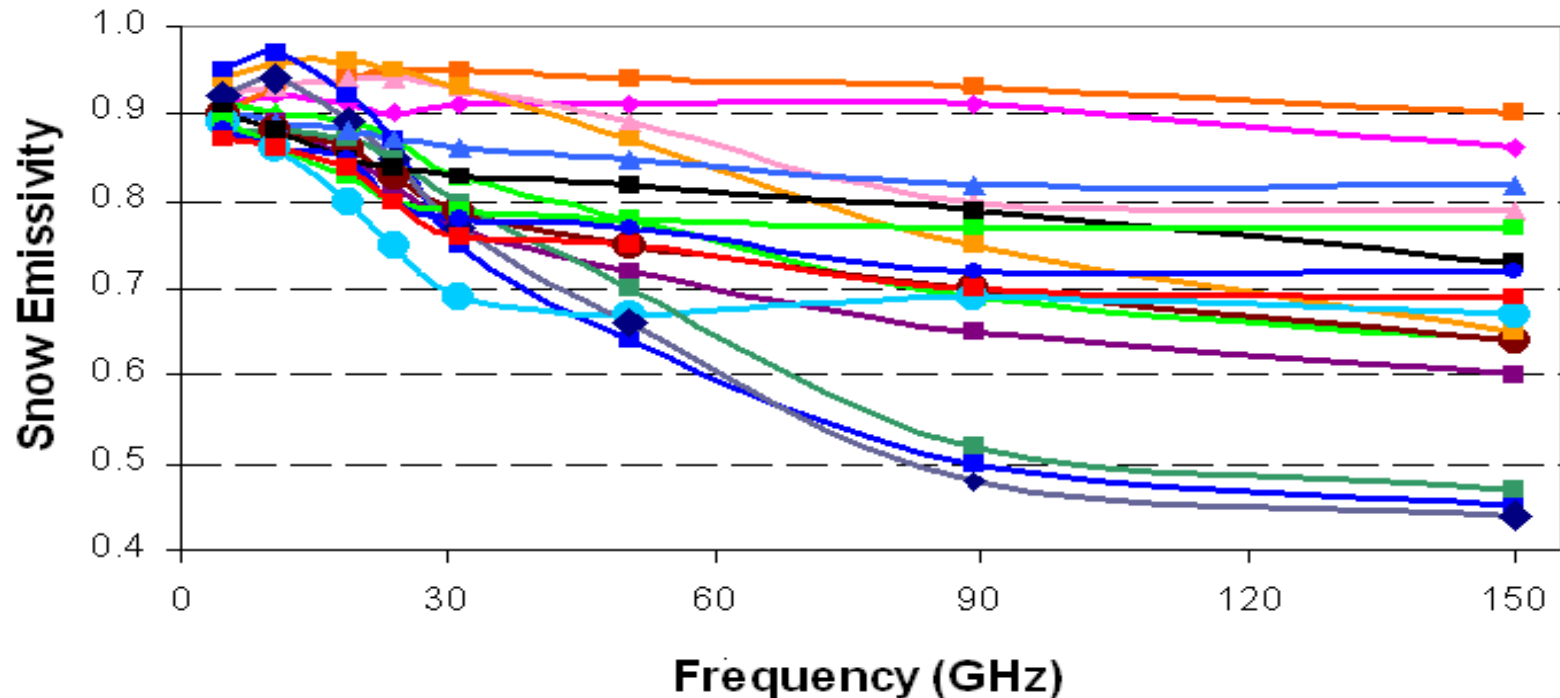
- **Open water** – two-scale roughness theory
- **Sea ice** – Coherent reflection
- **Canopy** – Four layer clustering scattering
- **Bare soil** – Coherent reflection and surface roughness
- **Snow/desert** – Random media

Weng et al (2001, JGR)



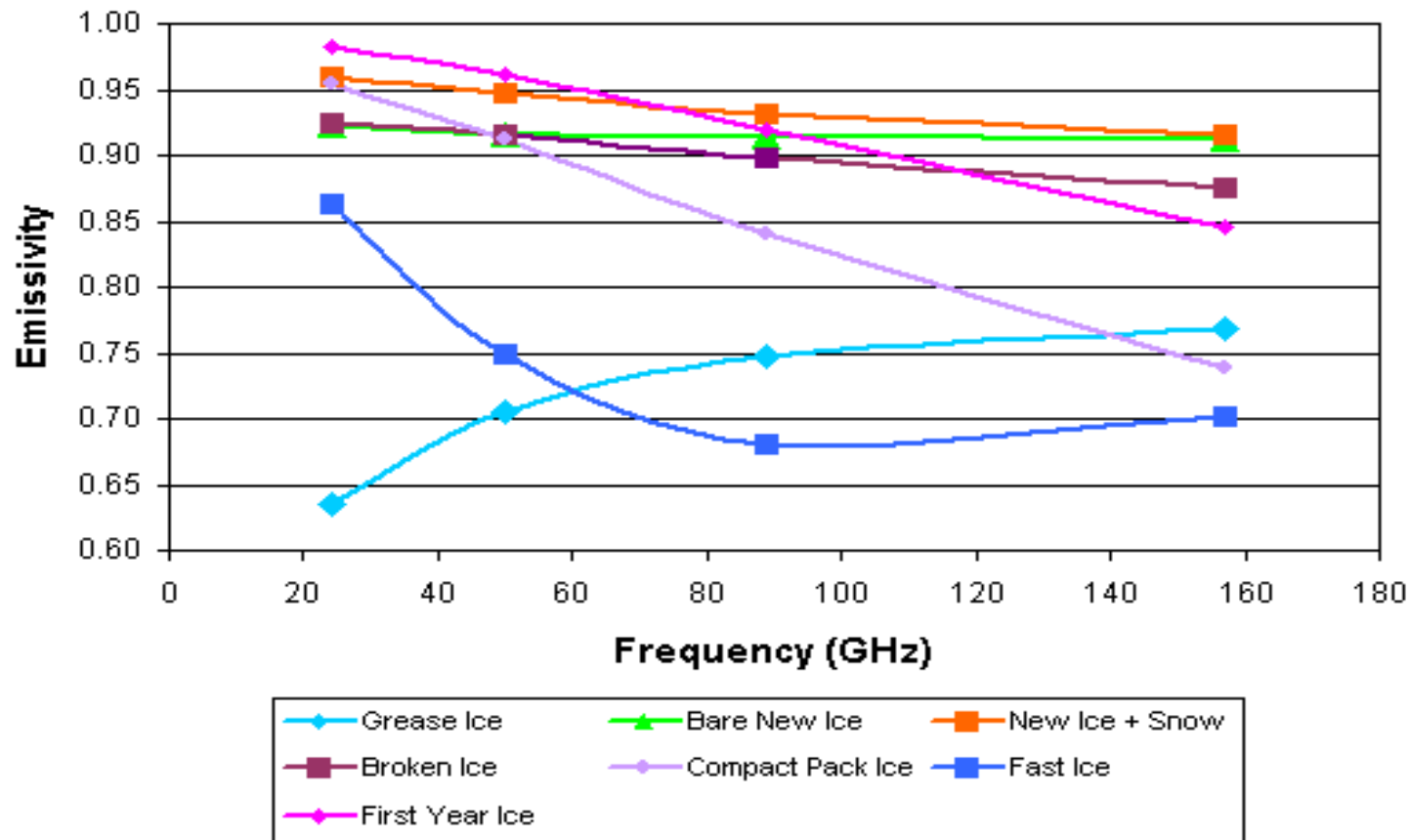
Algorithm Theoretical Basis (7/9)

Snow Emissivity:



Algorithm Theoretical Basis (8/9)

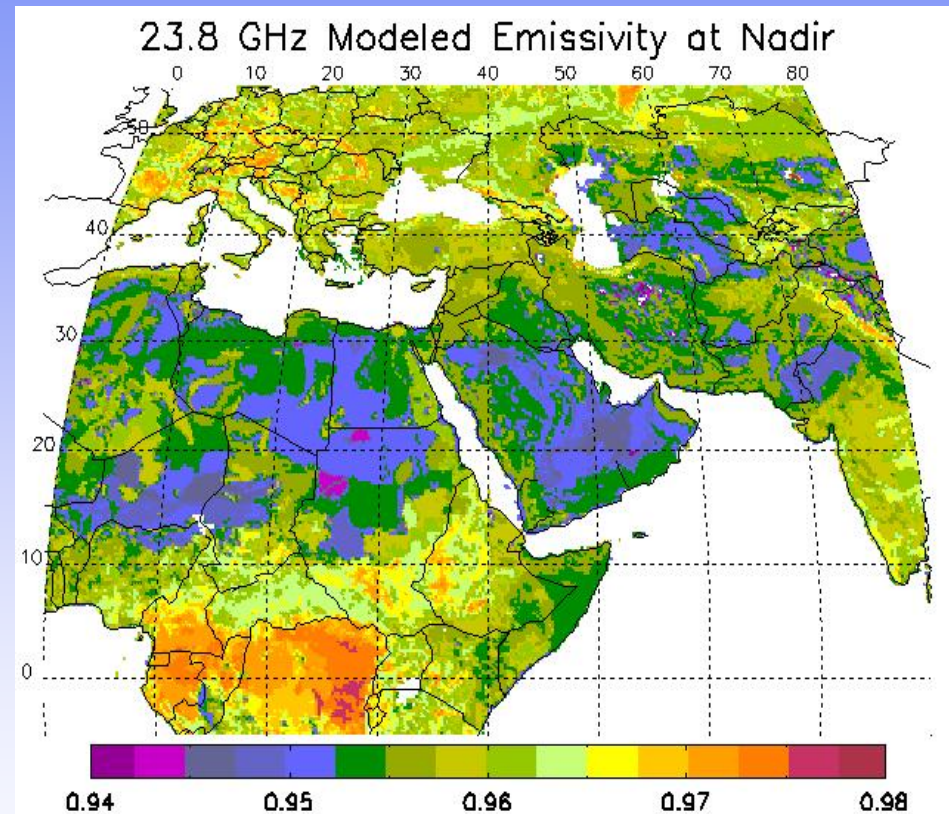
Sea Ice Emissivity Spectra



Algorithm Theoretical Basis (9/9)

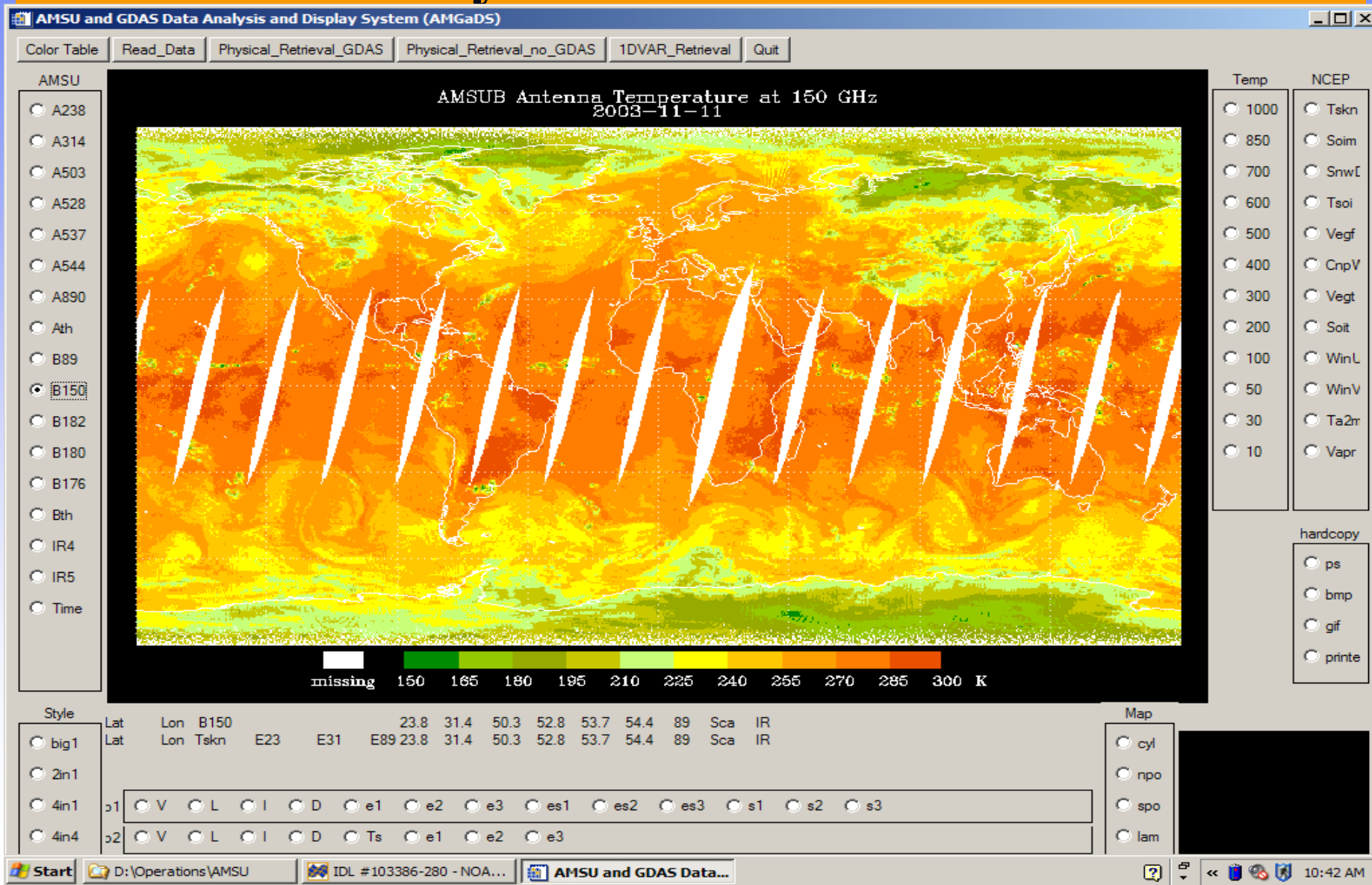
Desert Emissivity:

- NESDIS surface emissivity model outputs (Ruston & Baker, 2004)
- Clay/sand fraction from ISCLIP
- Soil moisture from AFWA model
- Vegetation from NDVI



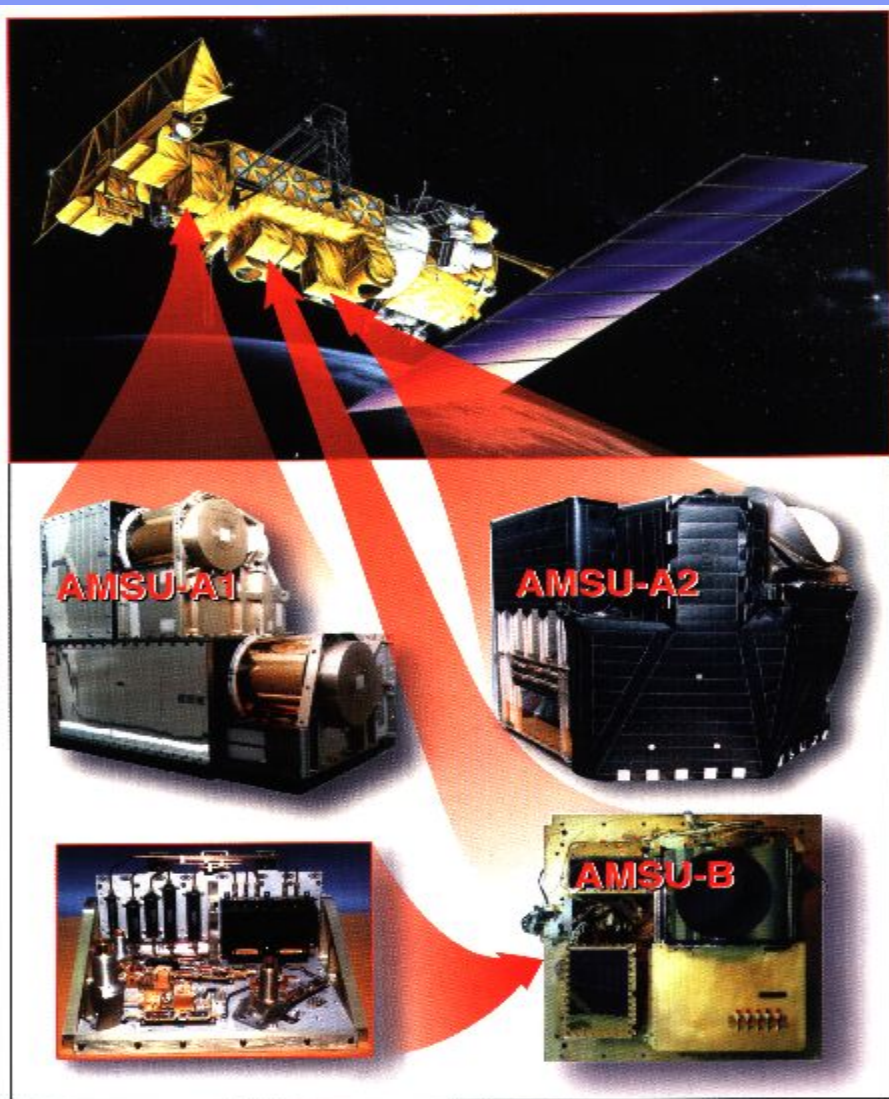


Microwave Integrated Retrieval System for AMSU





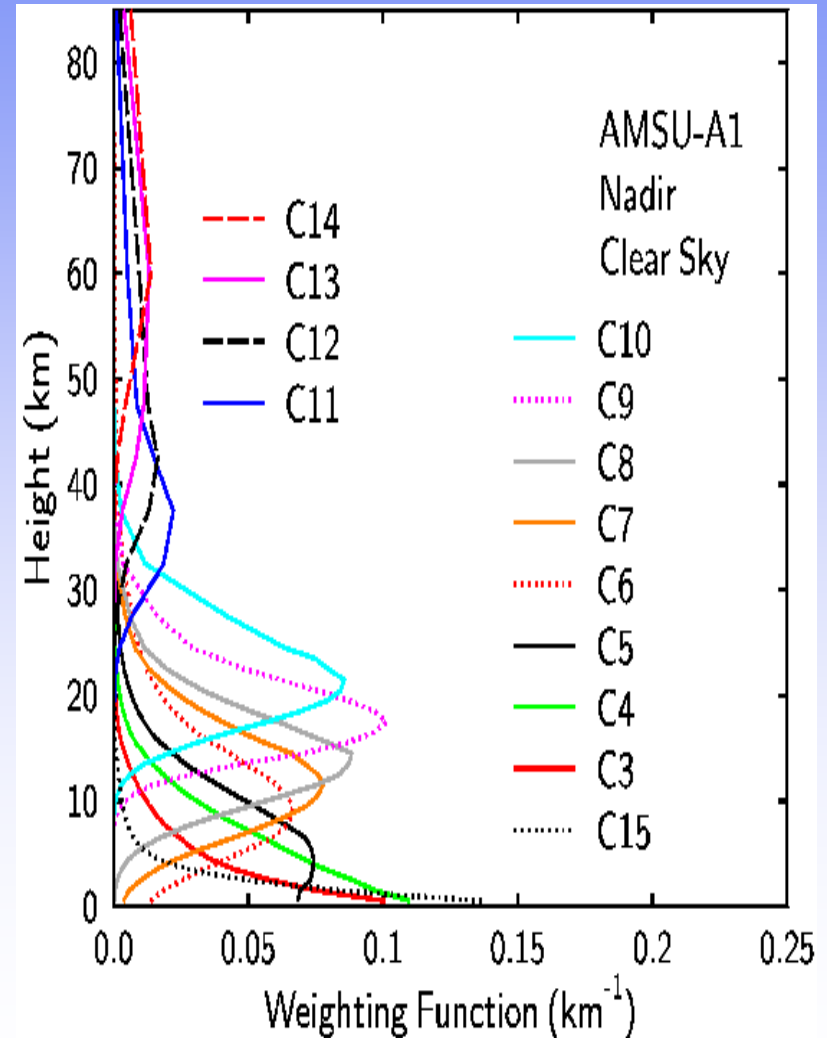
Advanced Microwave Sounding Unit



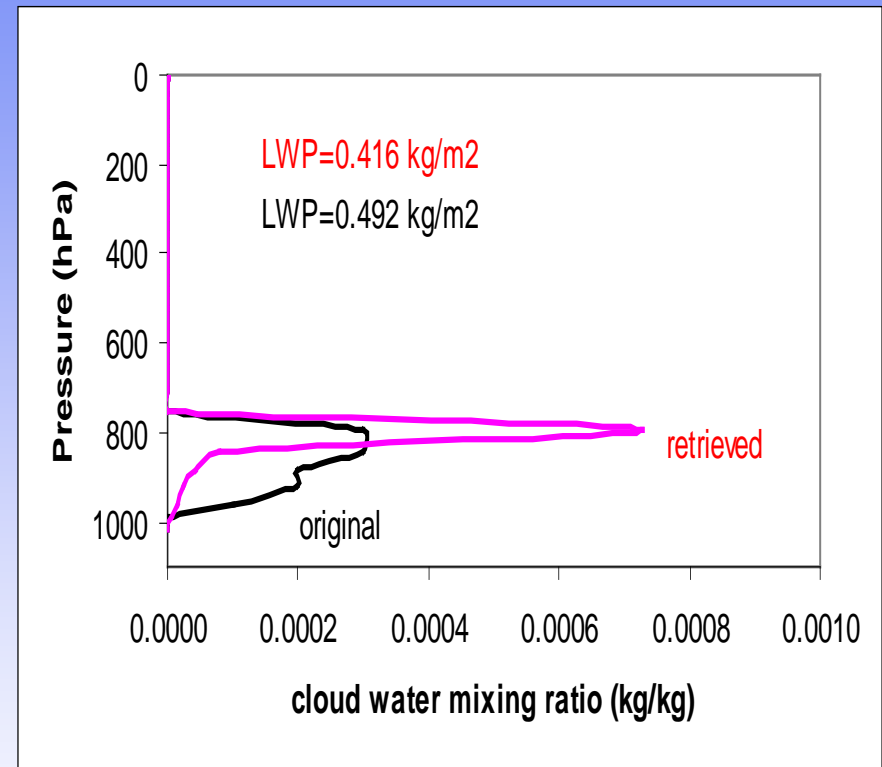
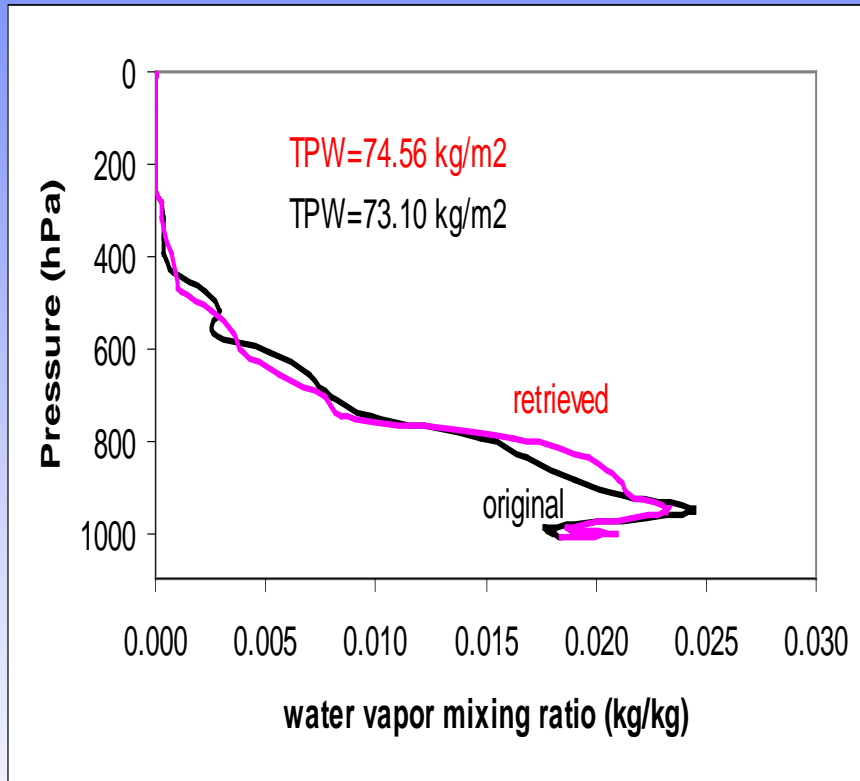
- Flown on NOAA-15 (May 1998), NOAA-16 (Sept. 2000) and NOAA-17 (June 2002) satellites
- Contains 20 channels:
 - AMSU-A
 - 15 channels
 - 23 – 89 GHz
 - AMSU-B
 - 5 channels
 - 89 – 183 GHz
- 4-hour temporal sampling:
 - 130, 730, 1030, 1330, 1930, 2230 LST

Advanced Microwave Sounding Unit

- AMSU measurement at each sounding channel responds primarily to emitted radiation within a layer, indicated by its weighting function
- The vertical resolution of sounding is dependent on the number of independent channel measurements
- Lower tropospheric channels are also affected by the surface radiation which is highly variable over land



Water Vapor and Cloud Water Profiles



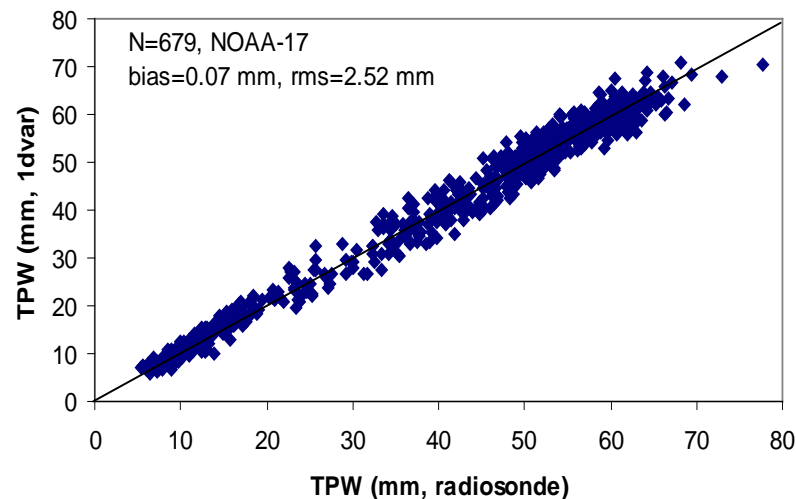
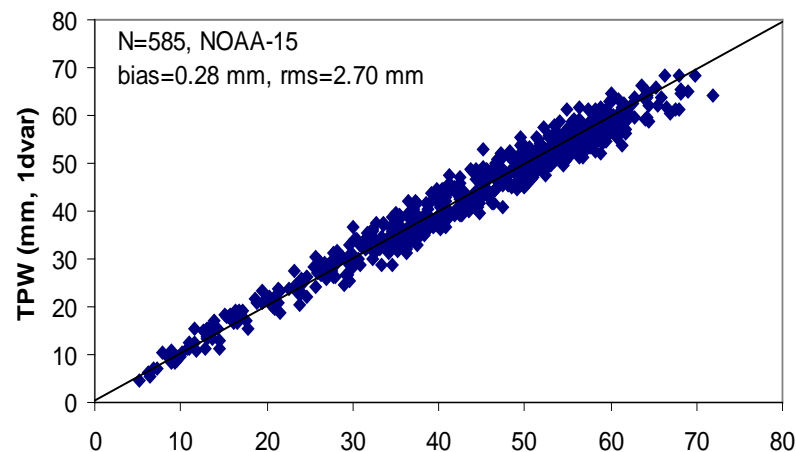
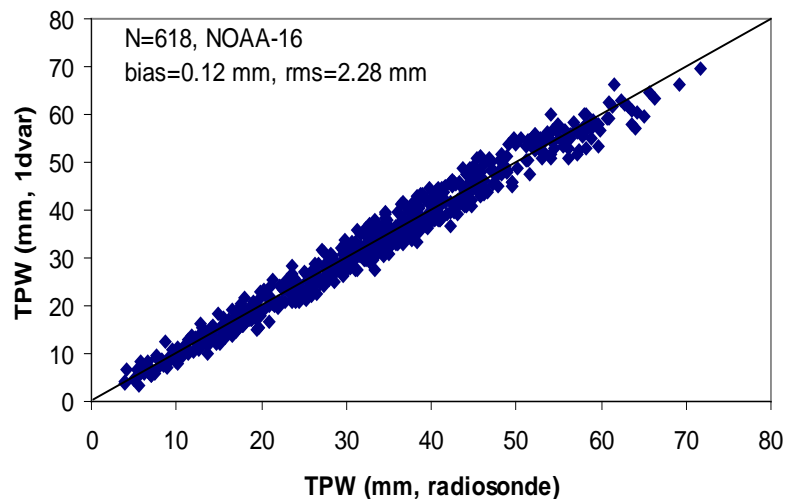
Standard atmosphere and cloudy layers between 800 and 950 hPa

Retrievals is based on simulated AMSU brightness temperatures at nadir



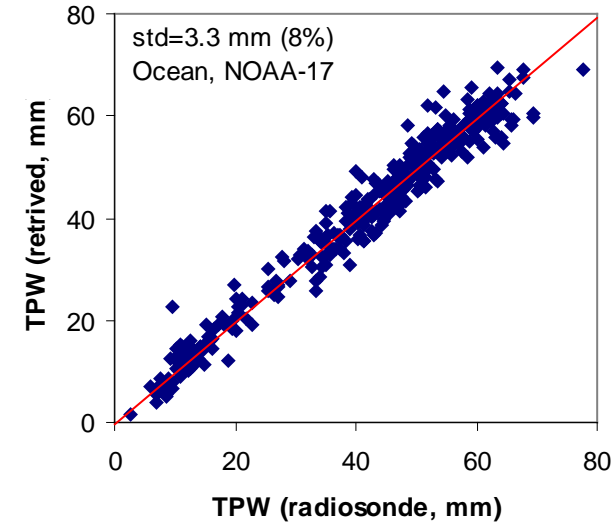
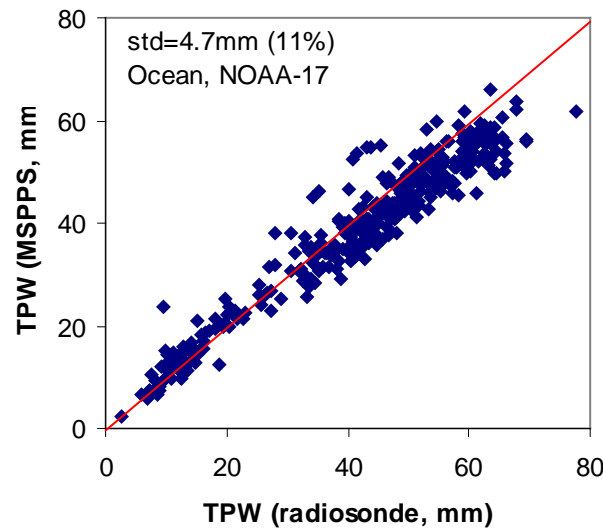
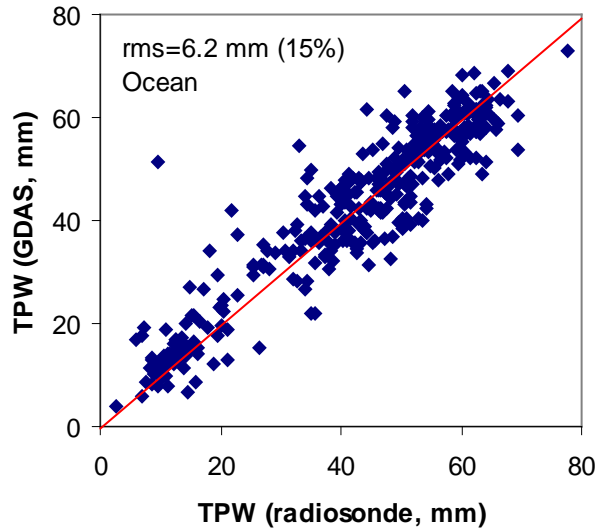
Vertically Integrated Water Vapor

Match-up TPW from radiosondes
and AMSU retrieval in 2002.





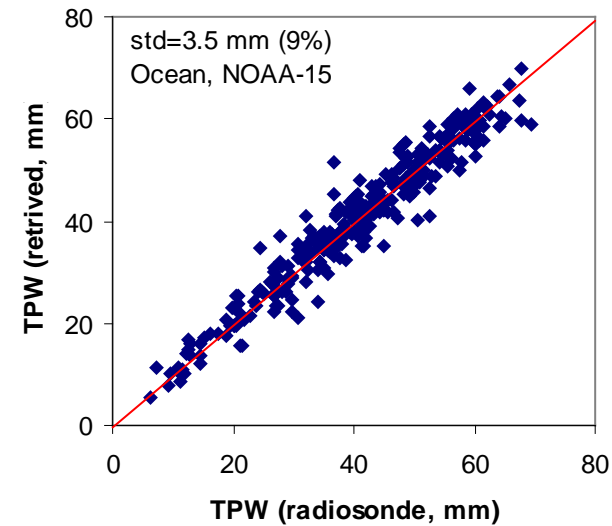
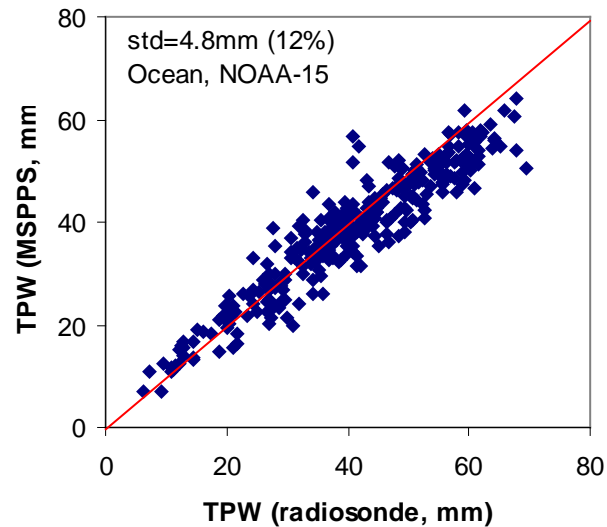
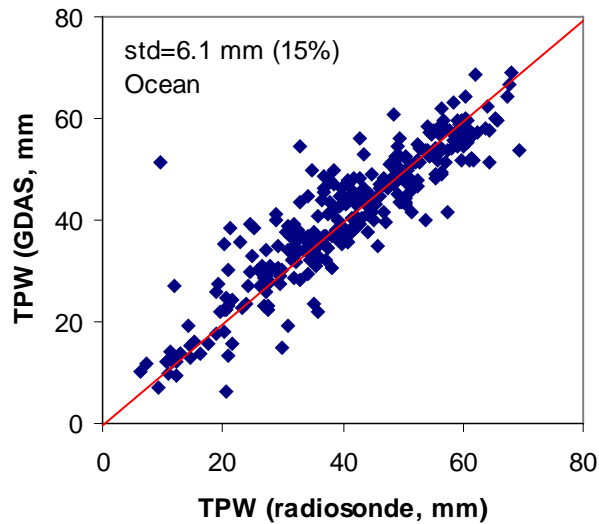
TPW Validation (NOAA-17)



In comparison to radiosonde measurements, MSPPS TPW product gives accuracy better than GDAS but is slightly biased. MIRS TPW is the best (no priori information).



TPW Validation (NOAA-15)

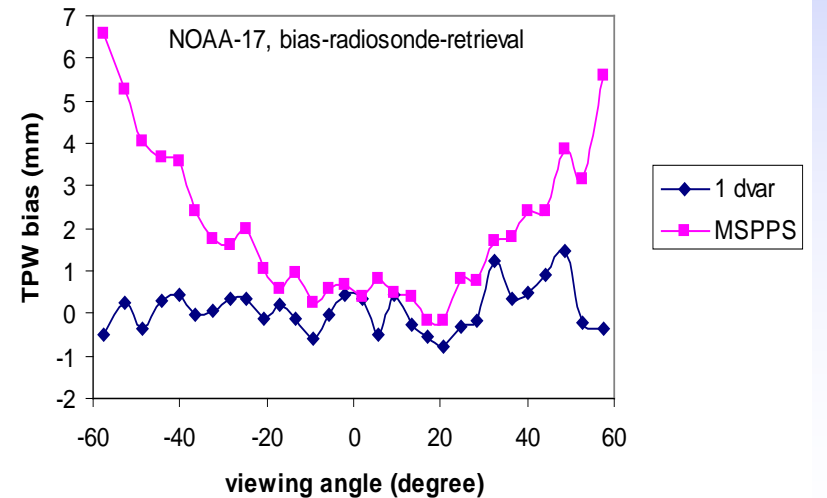
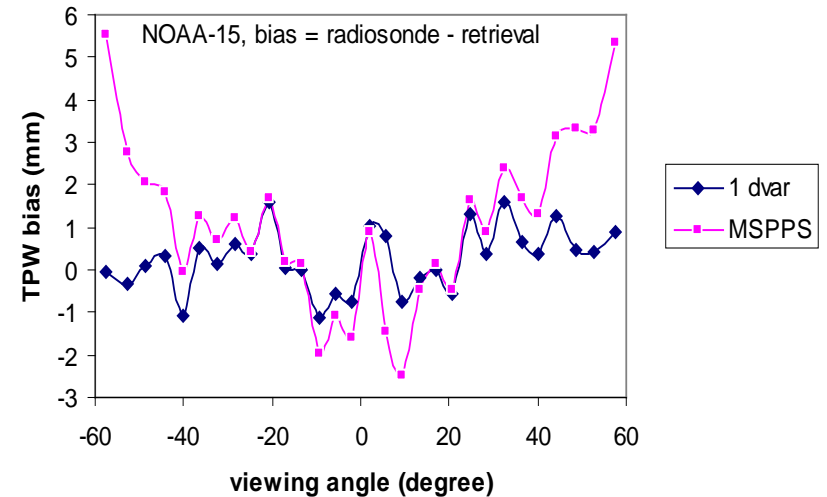
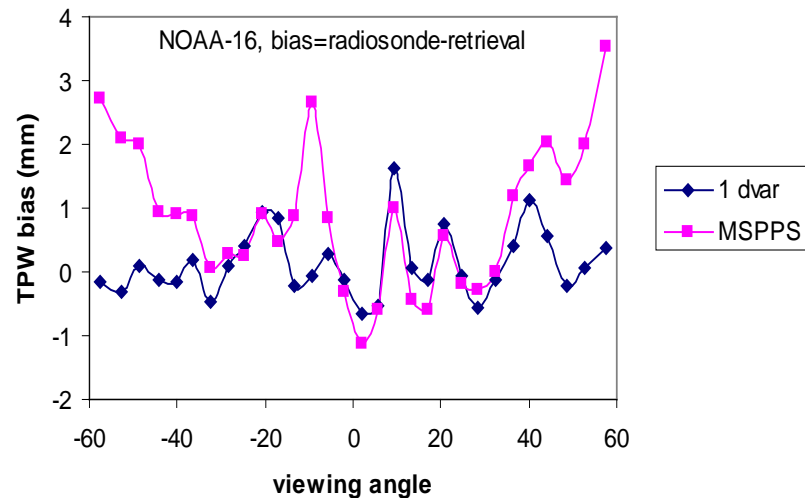


Retrieval Bias vs. Viewing Angles

Match-up TPW from radiosondes
and AMSU retrieval in 2002.

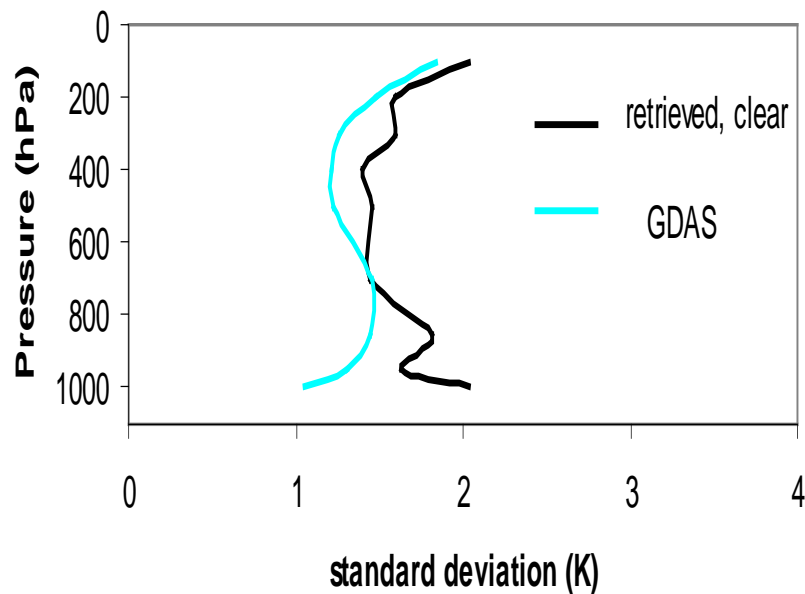
Bias variation to viewing angles.

Bias = radiosonde – AMSU

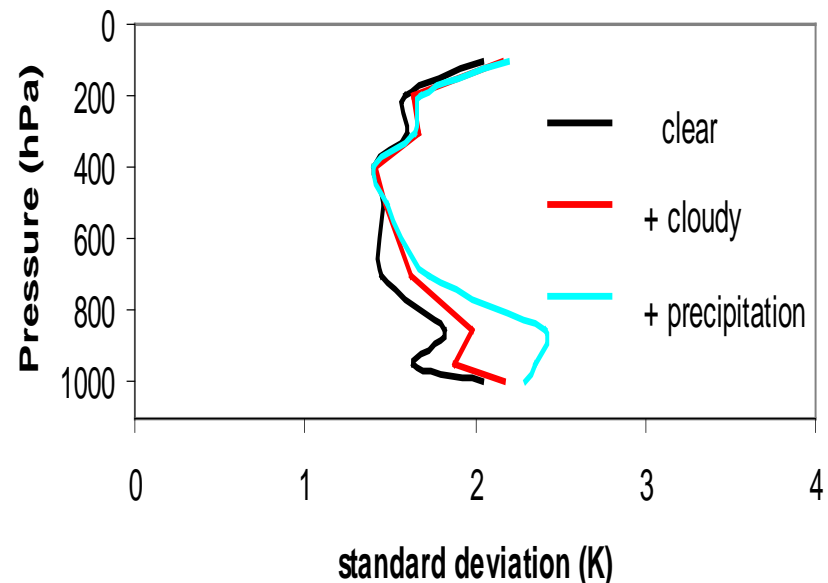


Temperature Validation (NOAA-17)

Comparison of temperature to radiosondes
ocean, NOAA-17



retrieved vs radiosondes temperature
ocean, NOAA-17

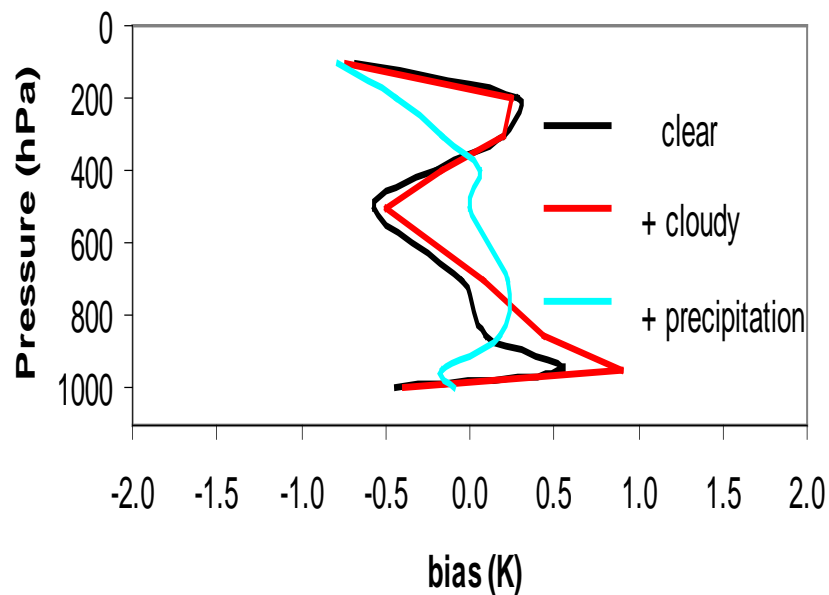


GDAS (1 x 1 deg) and radiosondes agree well. Clouds degrade the retrieval accuracy slightly. Clear samples = 357, clear+cloud samples = 501, clear+cloud+precipitation=552

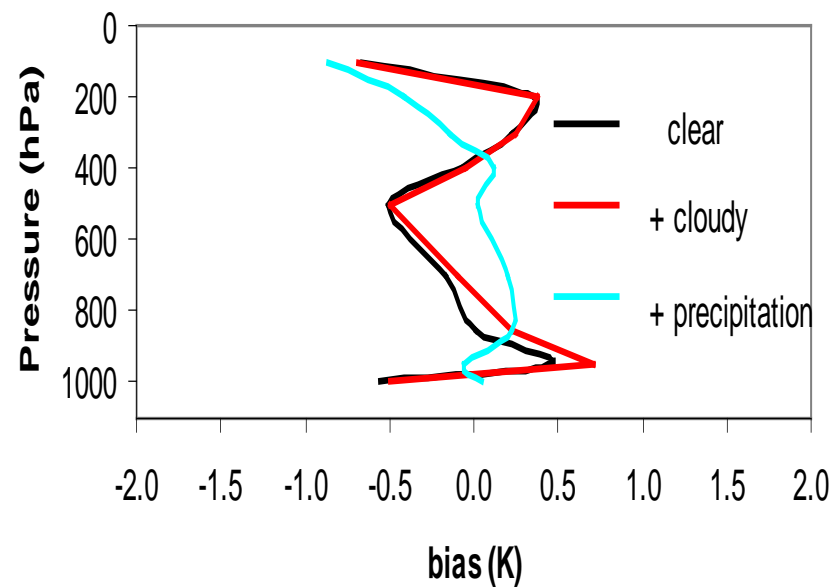


Temperature Validation (NOAA-17)

retrieved vs radiosondes temperature
ocean, NOAA-17

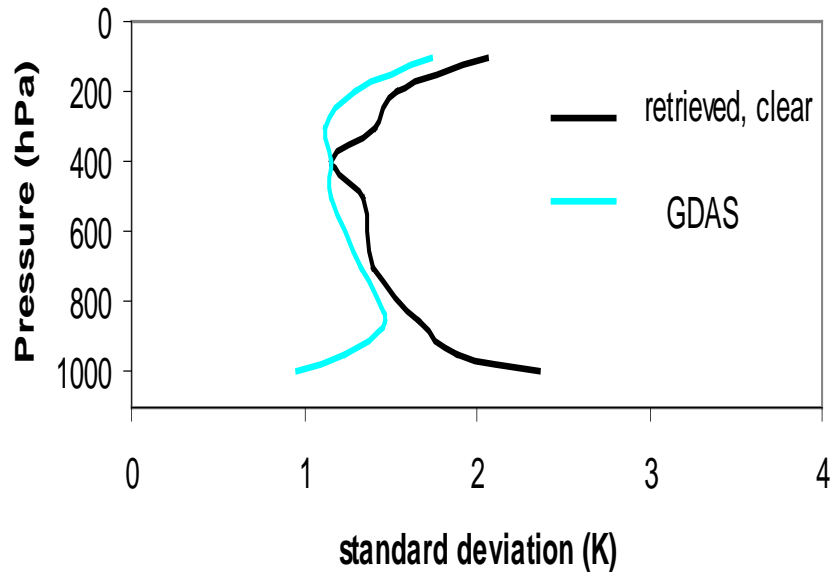


retrieved vs radiosondes temperature
ocean, NOAA-15

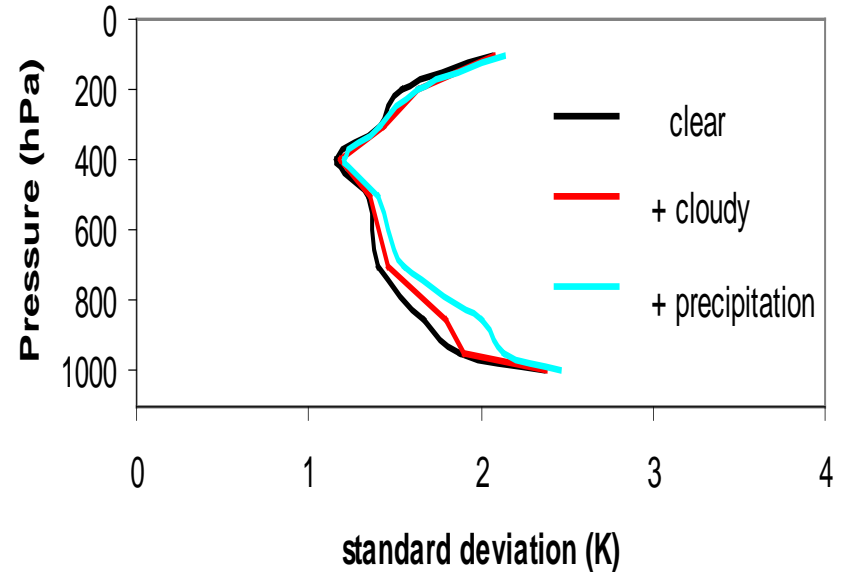


Temperature Validation (NOAA-15)

Comparison of temperature to radiosondes
ocean, NOAA-15



retrieved vs radiosondes temperature
ocean, NOAA-15

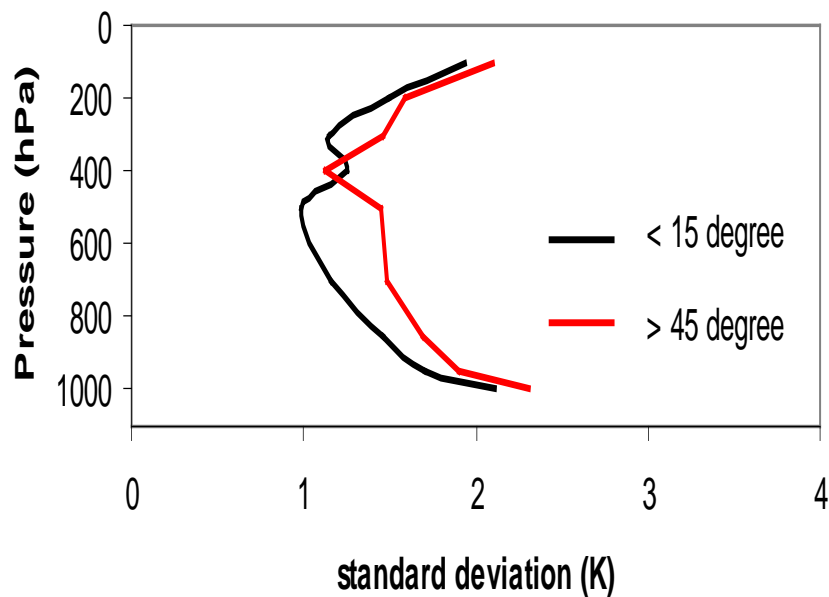


GDAS (1 x 1 deg) and radiosondes agree well. Clouds degrade the retrieval accuracy slightly. Clear samples = 278, clear+cloud samples = 386, clear+cloud+precipitation=416

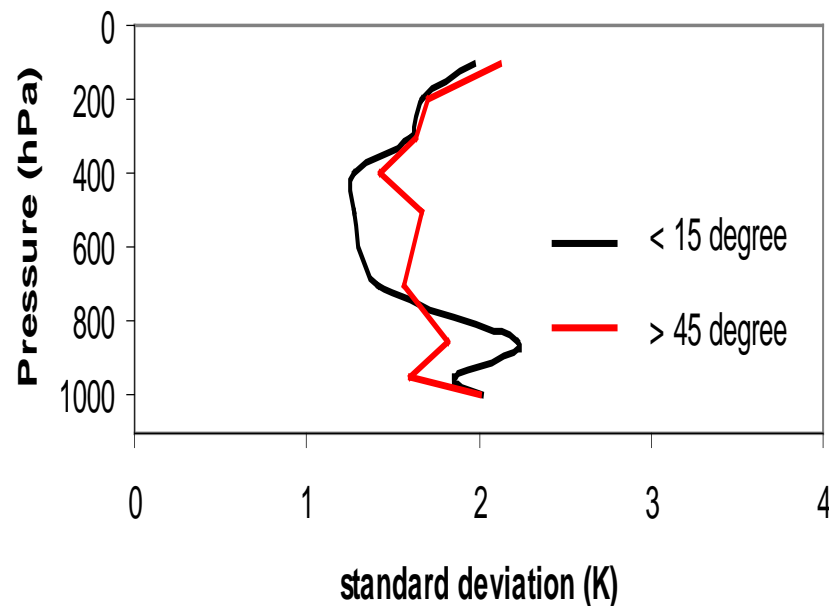


Temperature Accuracy (Nadir vs. off-Nadir)

Comparison of temperature to radiosonde
ocean, NOAA-15



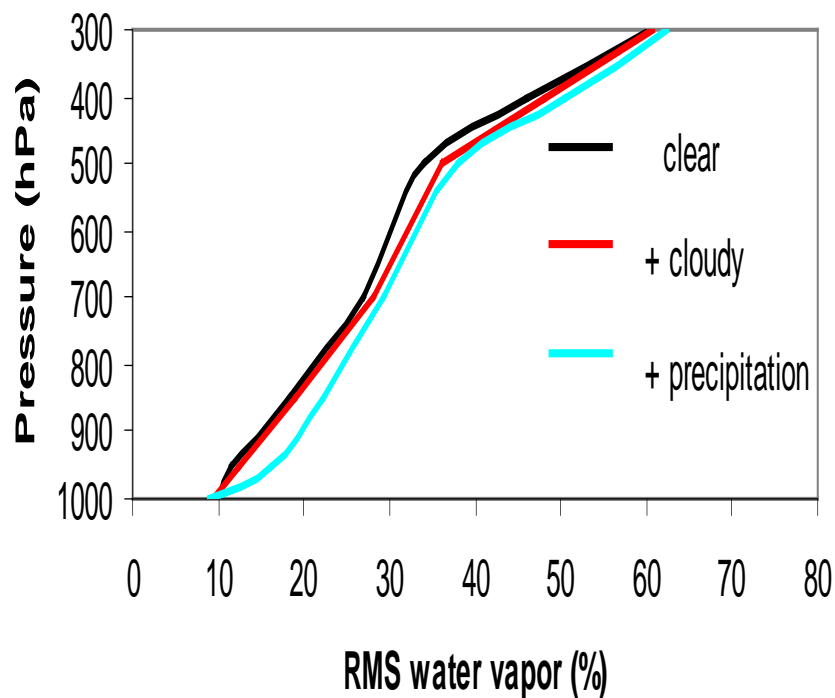
Comparison of temperature to radiosonde
ocean, NOAA-17



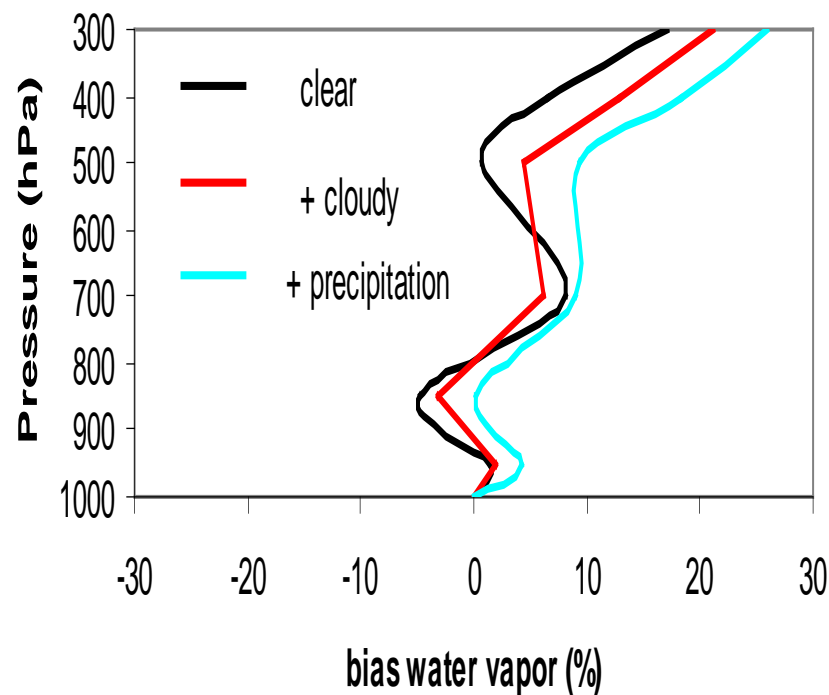


Validation for Water Vapor Profile

retrieved vs radiosondes water vapor profile
ocean, NOAA-17



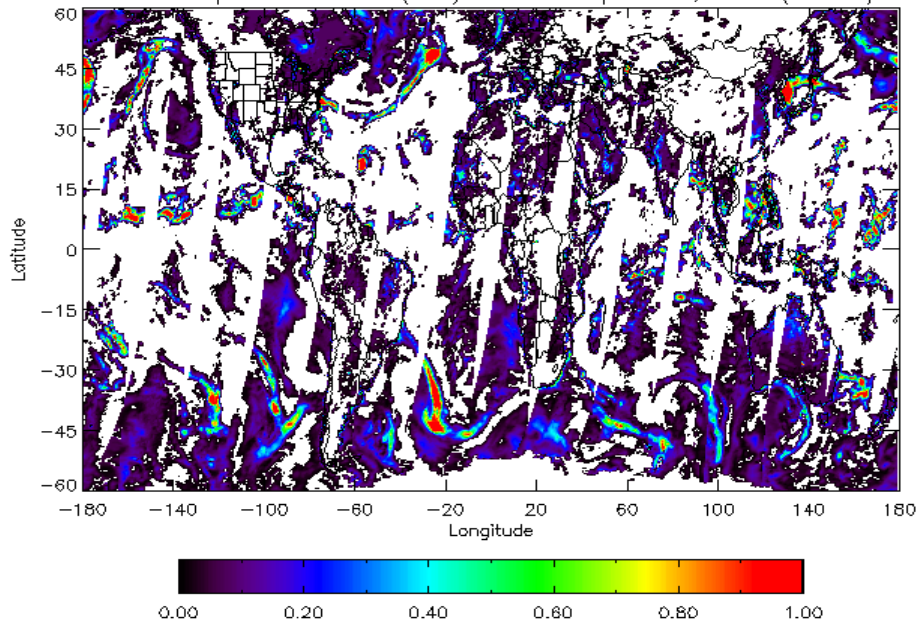
retrieved vs radiosondes water vapor profile
ocean, NOAA-17



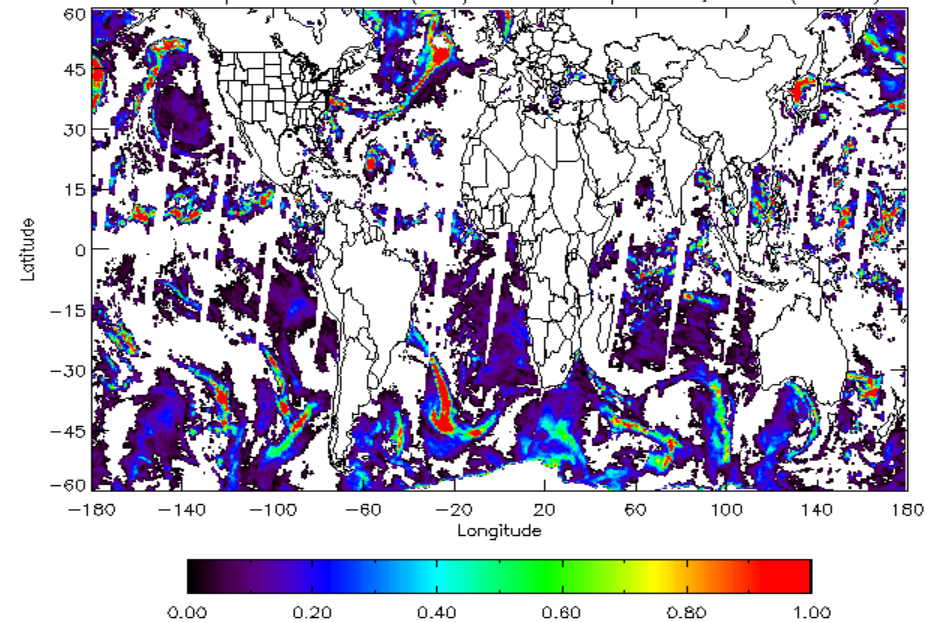


Cloud Liquid Water (MIRS vs. MSPPS)

Cloud Liquid Water Path (mm) on 12th September, 2003 (1D_var)



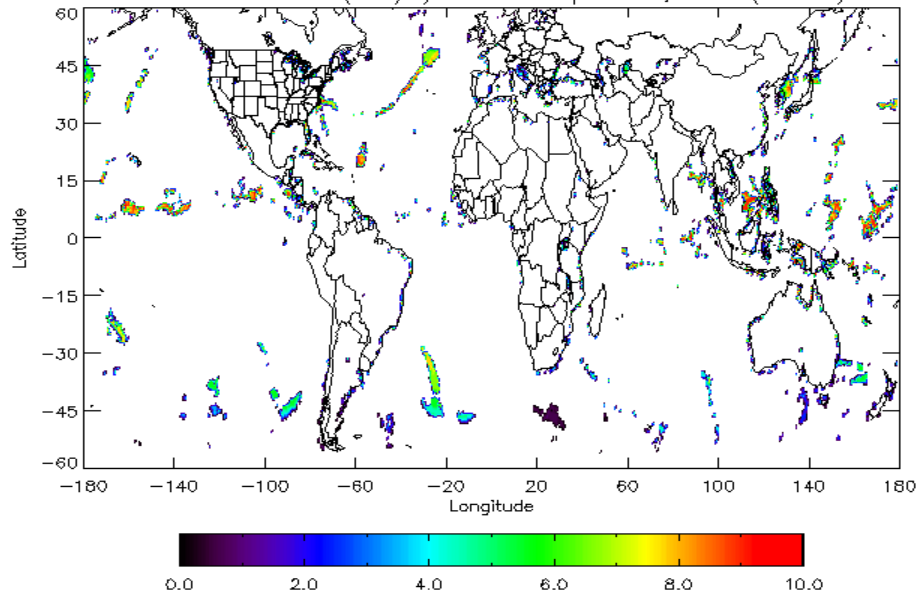
Cloud Liquid Water Path (mm) on 12th September, 2003 (MSPPS)



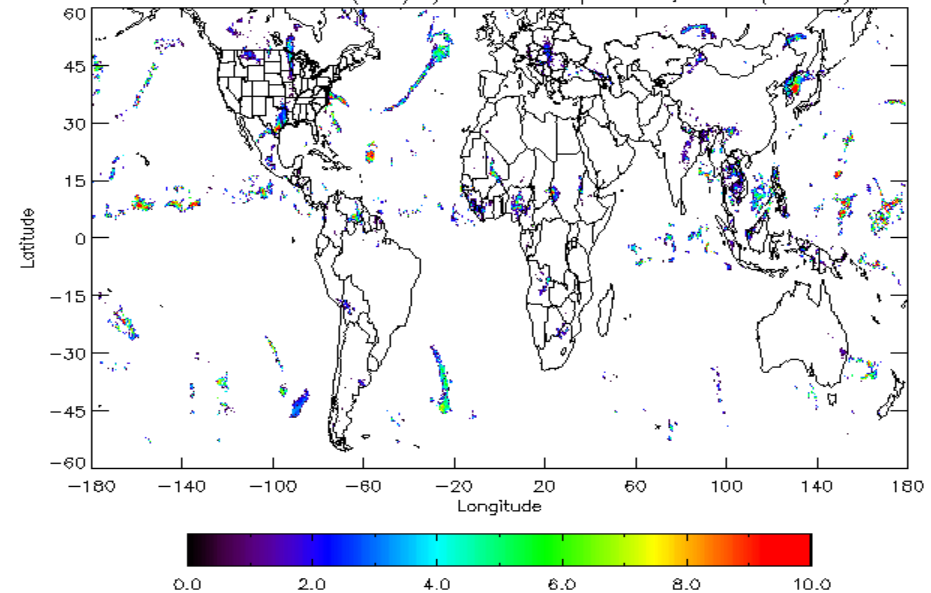


Precipitation (MIRS vs. MSPPS)

Surface rainrate (mm/h) on 12th September, 2003 (1D_var)



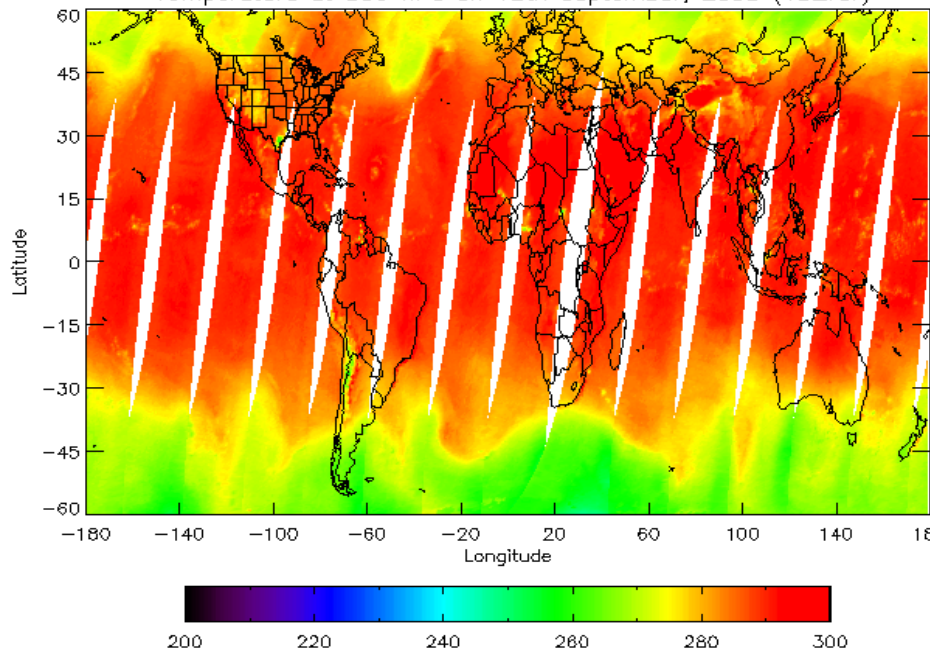
Surface rainrate (mm/h) on 12th September, 2003 (MSPPS)



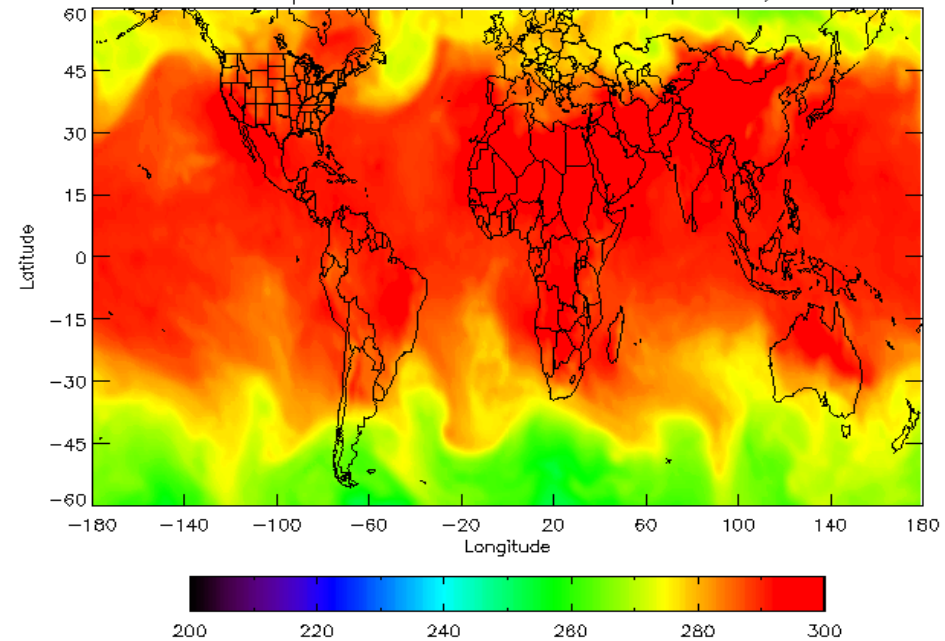


Temperature at 850 hPa (MIRS vs. GDAS)

Temperature at 850 hPa on 12th September, 2003 (1D_var)



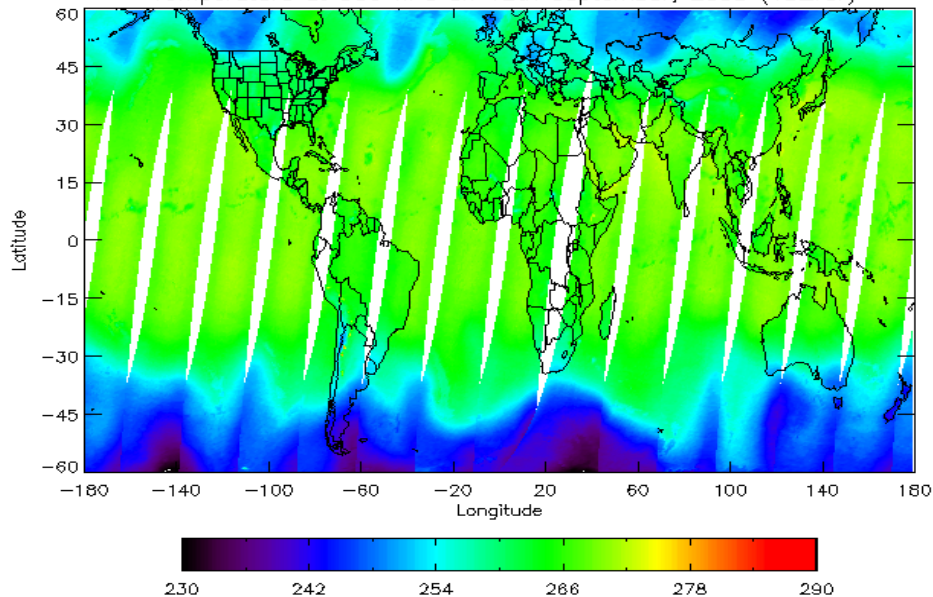
GDAS Temperature at 850 hPa on 12th September, 2003



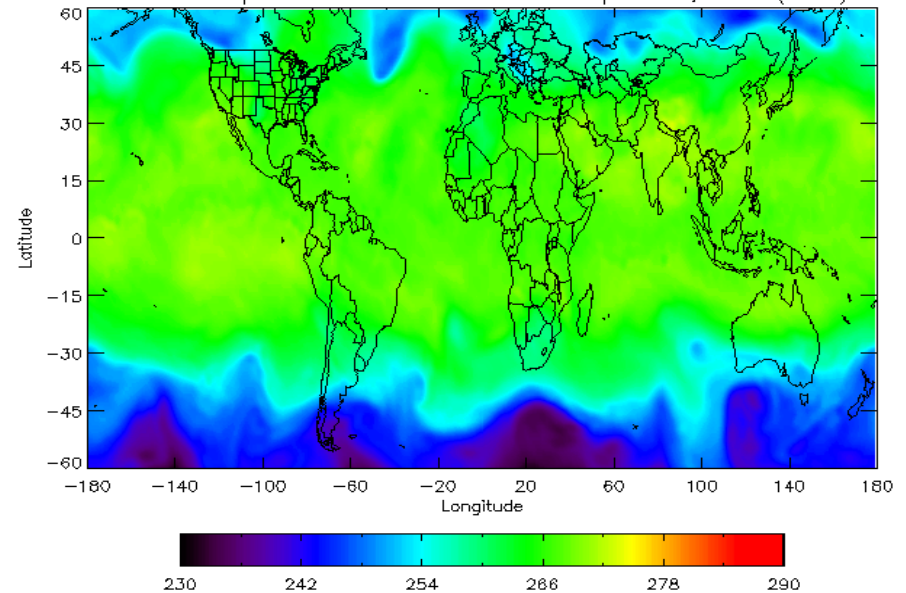


Temperature at 500 hPa (MIRS vs. GDAS)

Temperature at 500 hPa on 12th September, 2003 (1D_var)



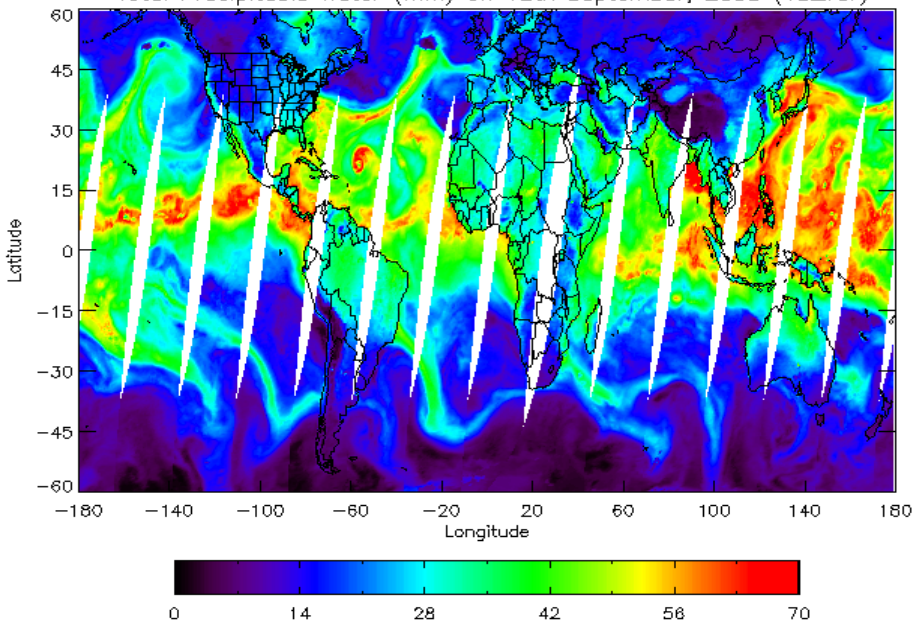
Isabel Temperature at 500 hPa on 12th September, 2003 (GDAS)



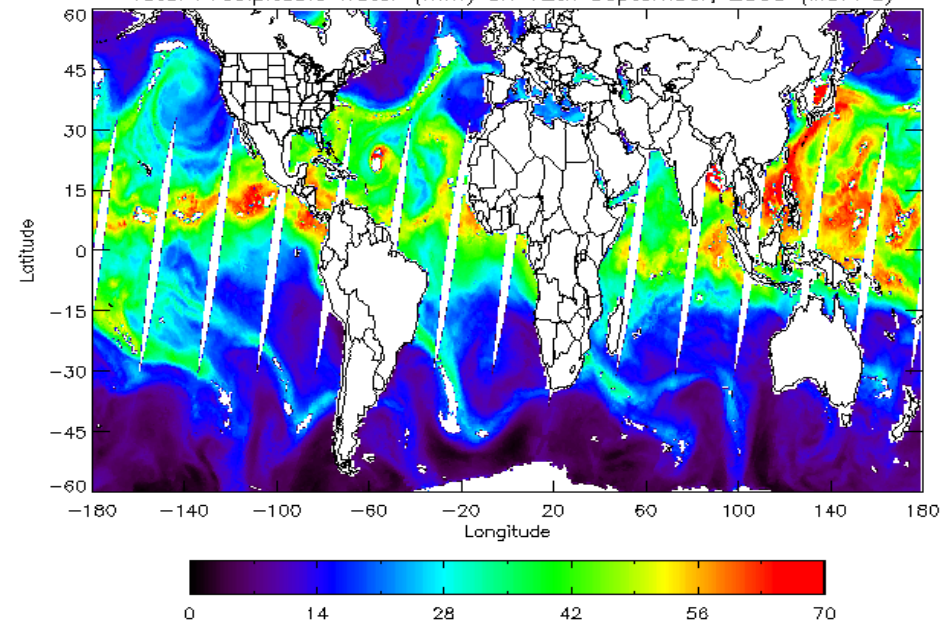


Total Precipitable Water (MIRS vs. MSPPS)

Total Precipitable Water (mm) on 12th September, 2003 (1D_var)

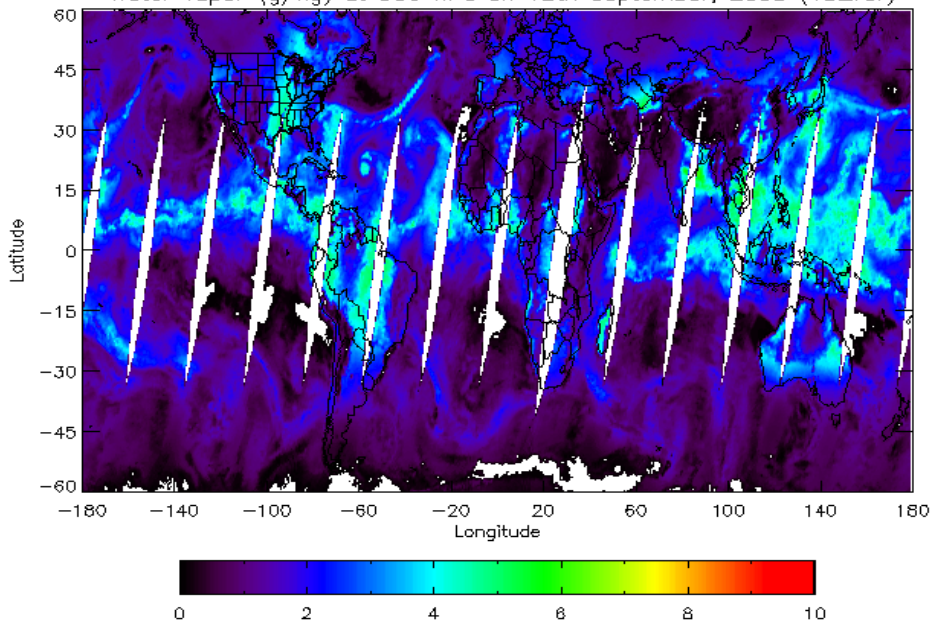


Total Precipitable Water (mm) on 12th September, 2003 (MSPPS)

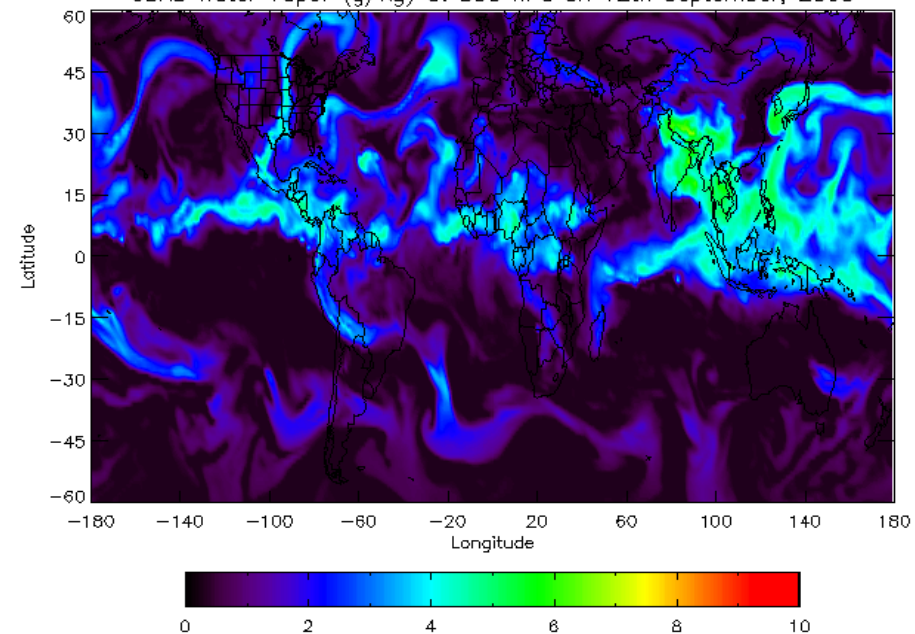


Water Vapor at 500 hPa (MIRS vs. GDAS)

Water vapor (g/kg) at 500 hPa on 12th September, 2003 (1D_var)



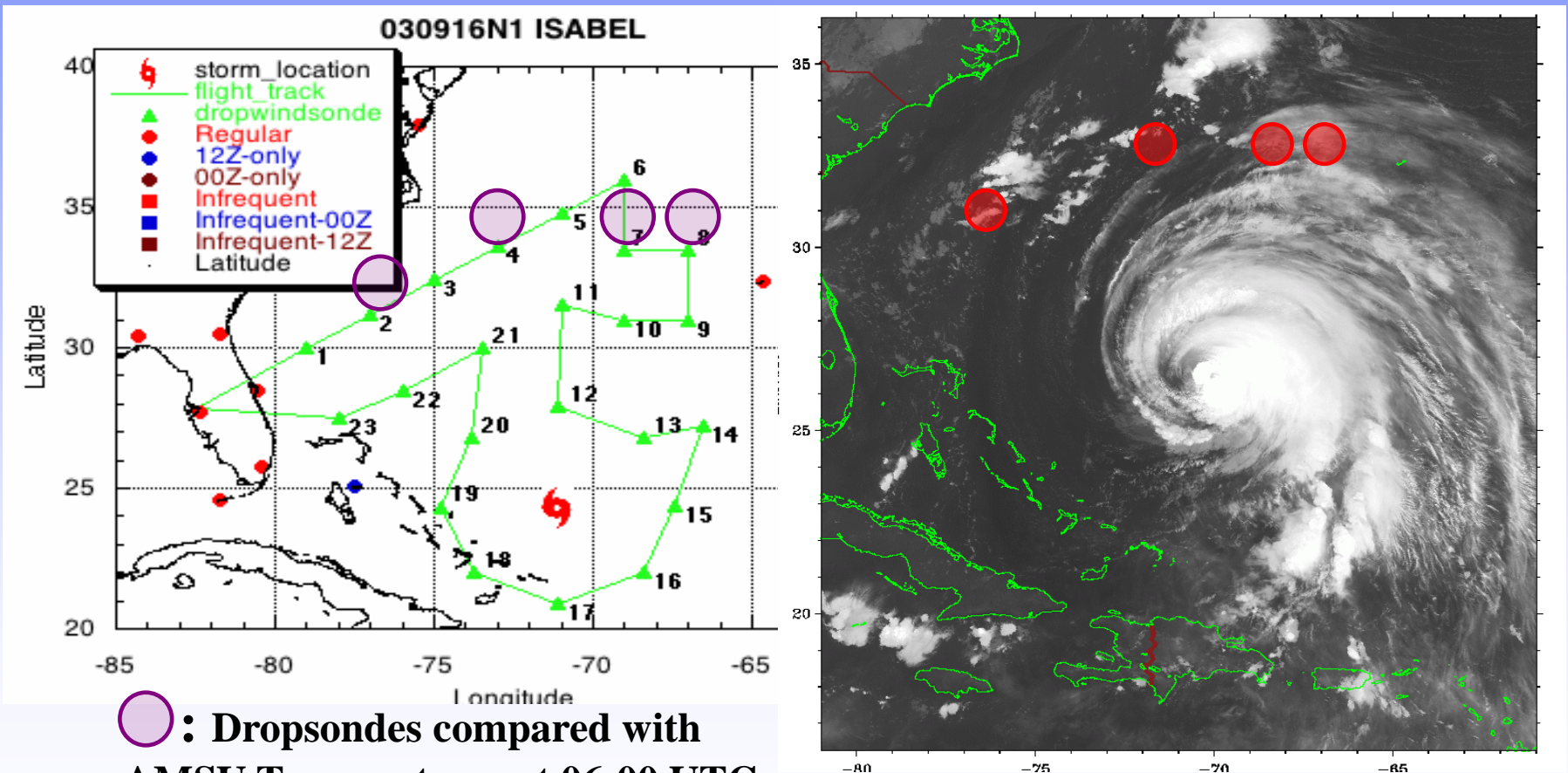
GDAS Water Vapor (g/kg) at 500 hPa on 12th September, 2003





Aircraft Dropsondes in Hurricane Isabel

Aircraft: N49RF Takeoff: 09/16/0530Z Land: 09/16/1300Z

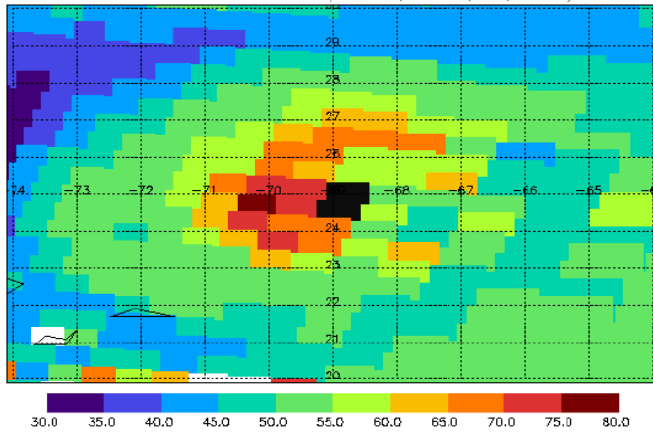




Water Vapor, Cloud Water and Rain Rate

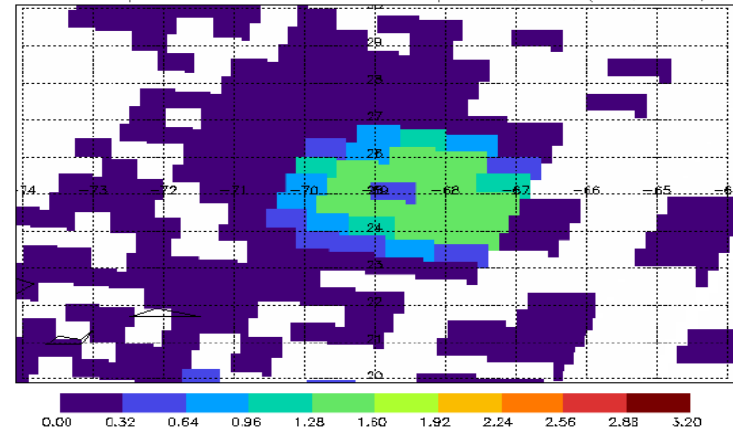
TPW

TPW for Isabel on 15th September, 2003 (N16, 1dvar)



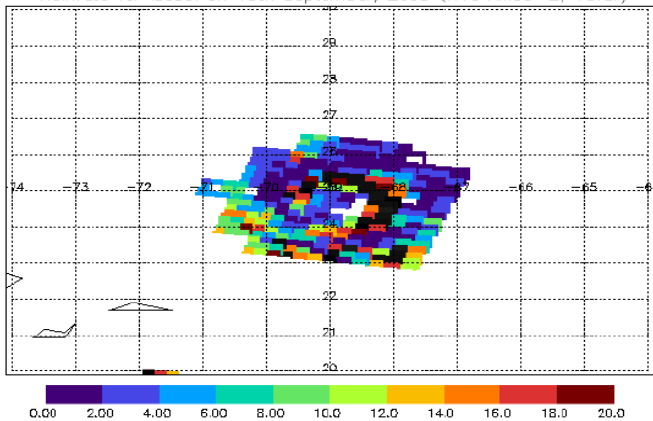
CLW

Cloud liquid water for Isabel on 15th September, 2003 (N16, 1dvar)



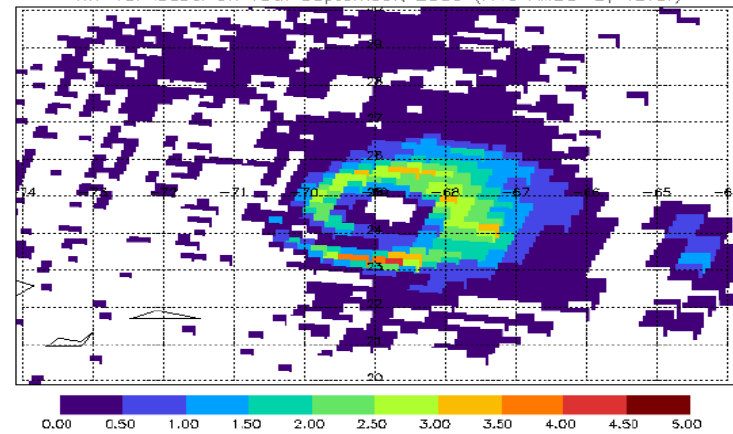
Rain Rate

Rainrate for Isabel on 15th September, 2003 (N16 AMSU-B, 1dvar)



IWP

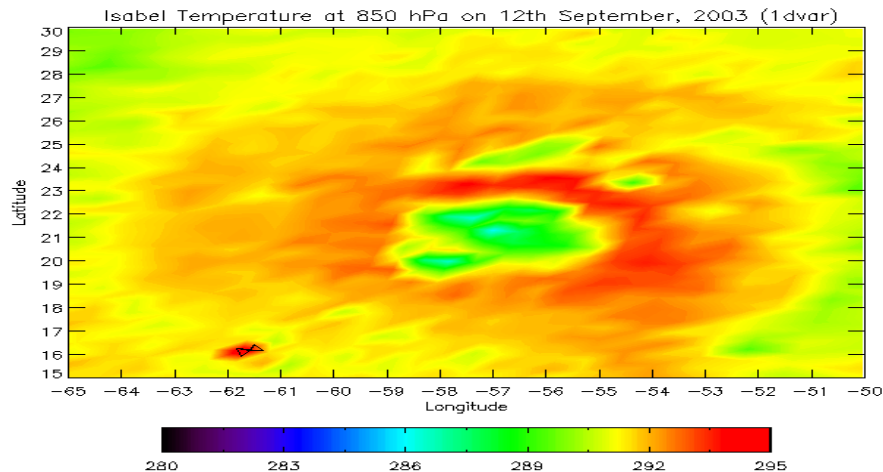
IWP for Isabel on 15th September, 2003 (N16 AMSU-B, 1dvar)



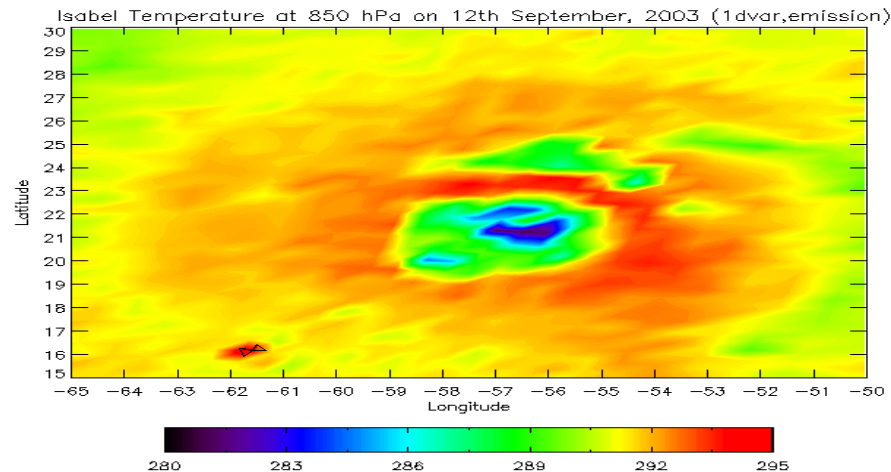


Impacts of Forward Models

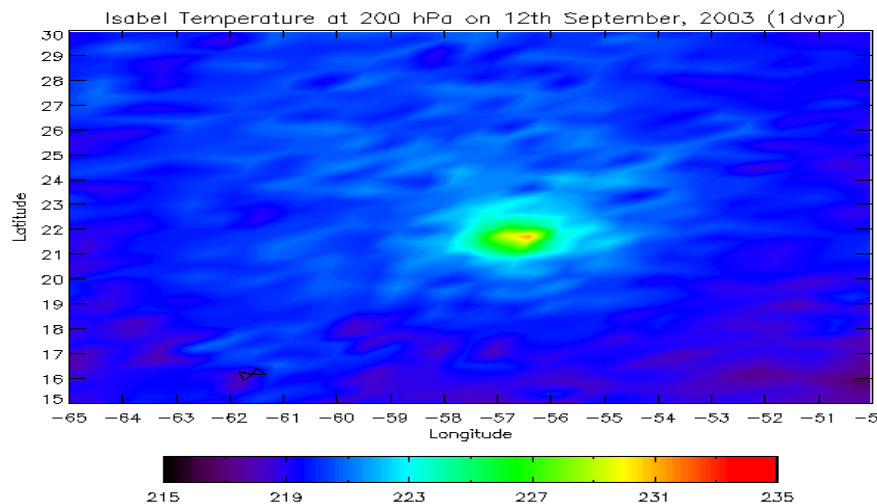
T(850hPa) – Scattering



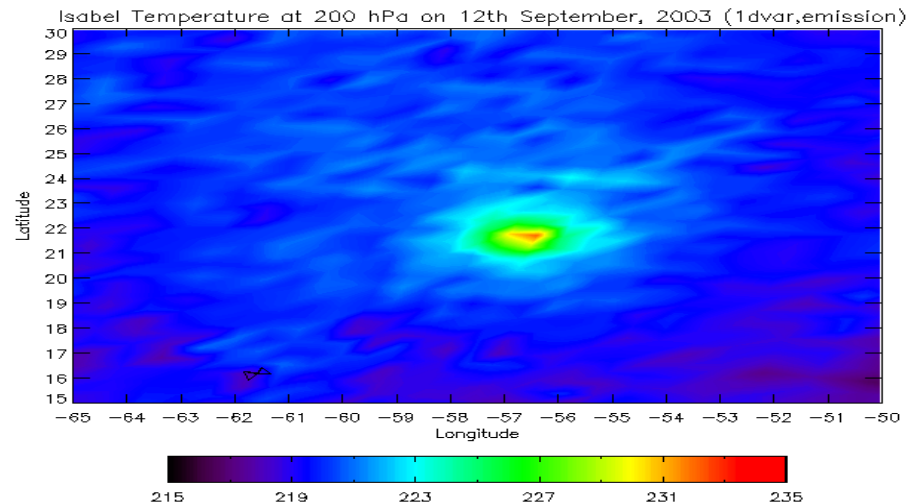
T(850hPa) – Emission only



T(200hPa) – Scattering

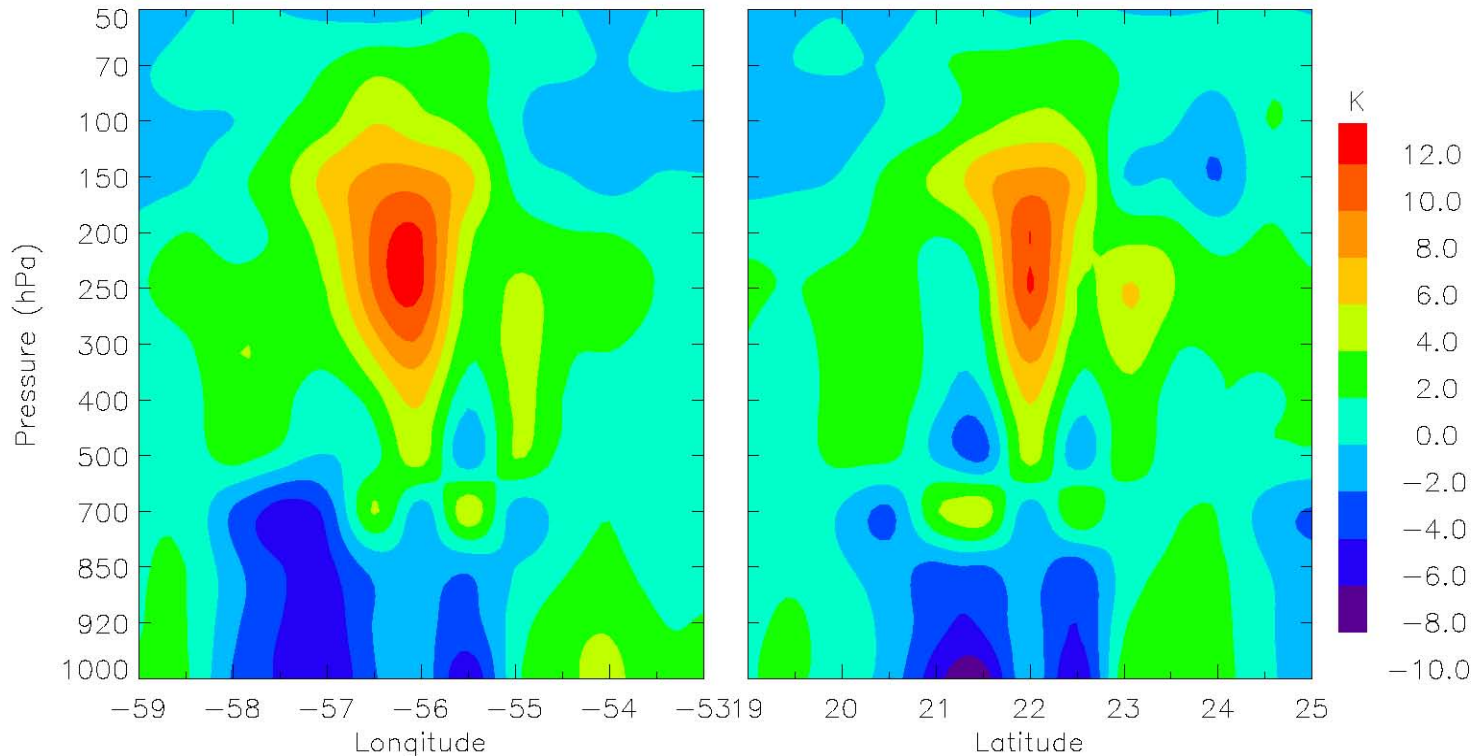


T(200hPa) – Emission only



Temperature Anomaly

With Cloud/Precipitation Scattering

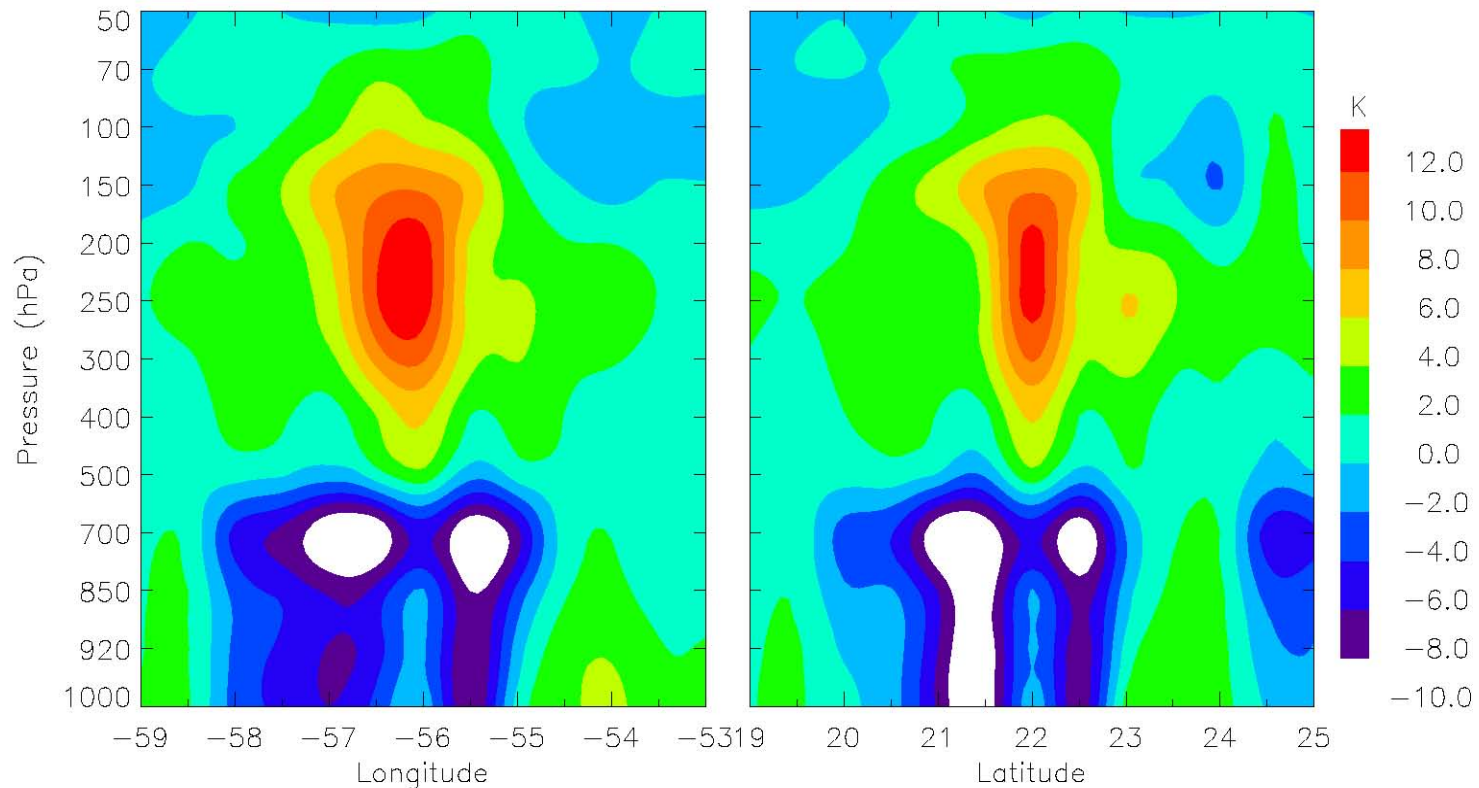


Vertical cross section of temperature anomalies at 06:00 UTC 09/12/2003. Left panel: west-east cross section along 22°N, and right panel: south-north cross section along 56°W for Hurricane Isabel

$$\mu \frac{d\mathbf{I}(\tau, \Omega)}{d\tau} = -\mathbf{I}(\tau, \Omega) + \frac{\omega}{4\pi} \int_0^{4\pi} \mathbf{M}(\tau, \Omega, \Omega') \mathbf{I}(\tau, \Omega') d\Omega' + (1 - \omega) \mathbf{S}_t$$

Temperature Anomaly

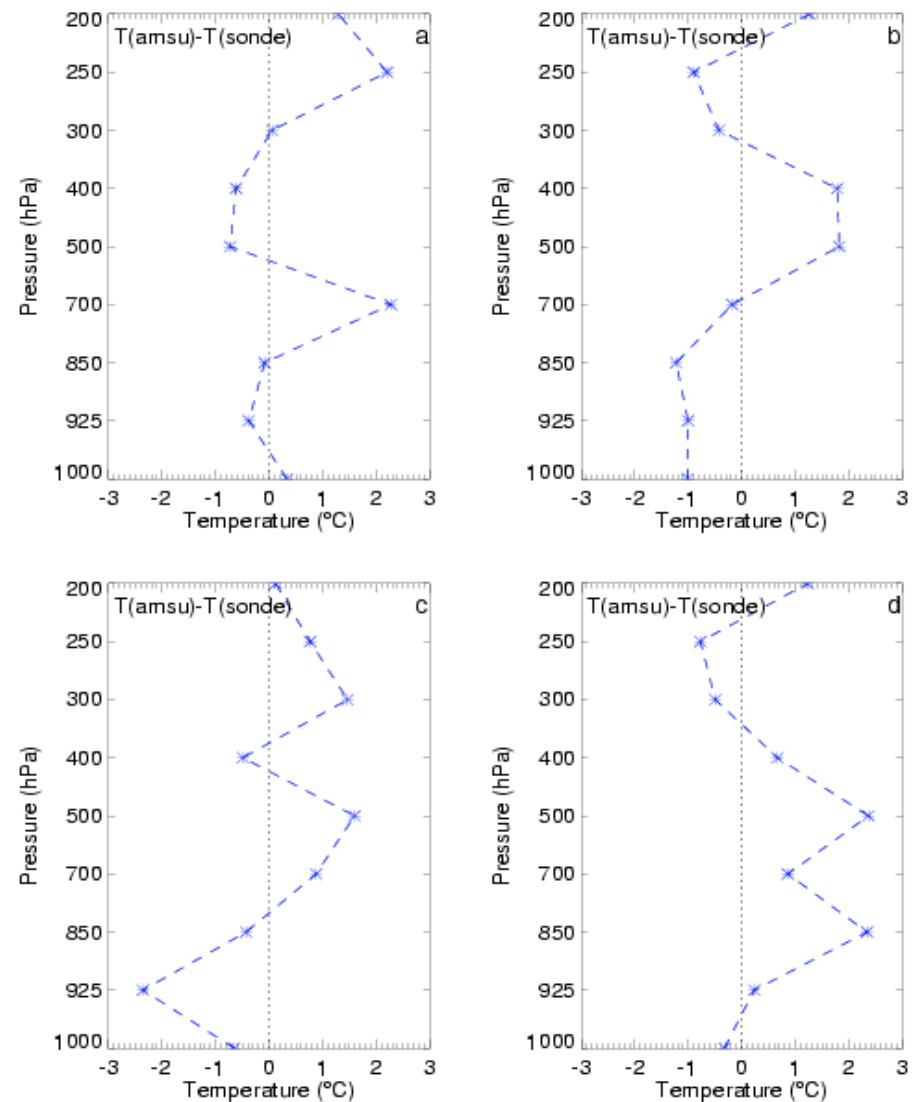
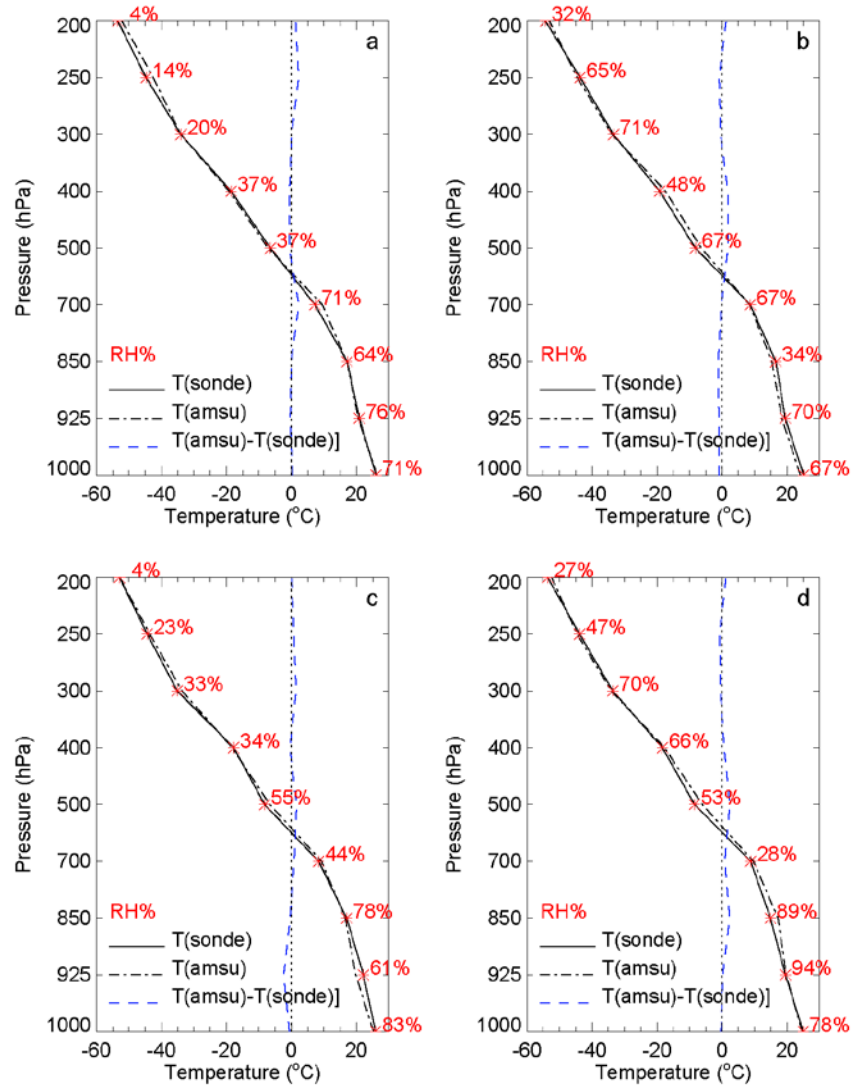
Without Cloud/Precipitation Scattering



Vertical cross section of temperature anomalies at 06:00 UTC 09/12/2003. Left panel: west-east cross section along 22°N, and right panel: south-north cross section along 56°W for Hurricane Isabel

$$\mu \frac{d\mathbf{I}(\tau, \Omega)}{d\tau} = -\mathbf{I}(\tau, \Omega) + (1 - \omega)\mathbf{S}_t$$

Intercomparison with Dropsondes

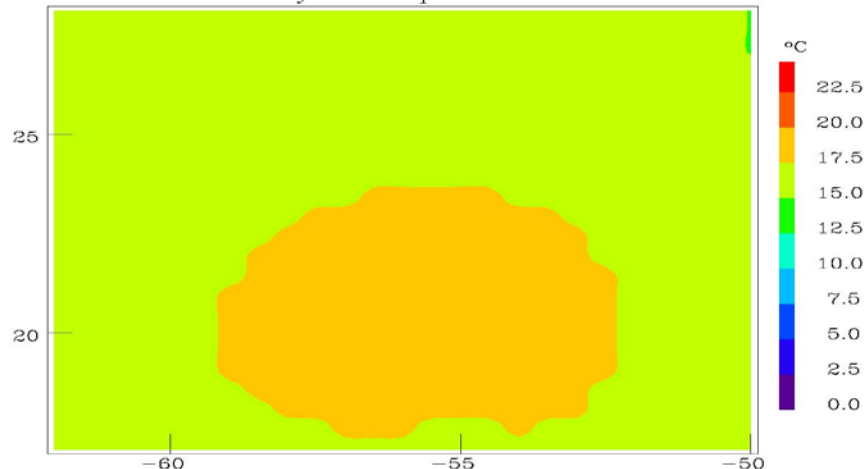




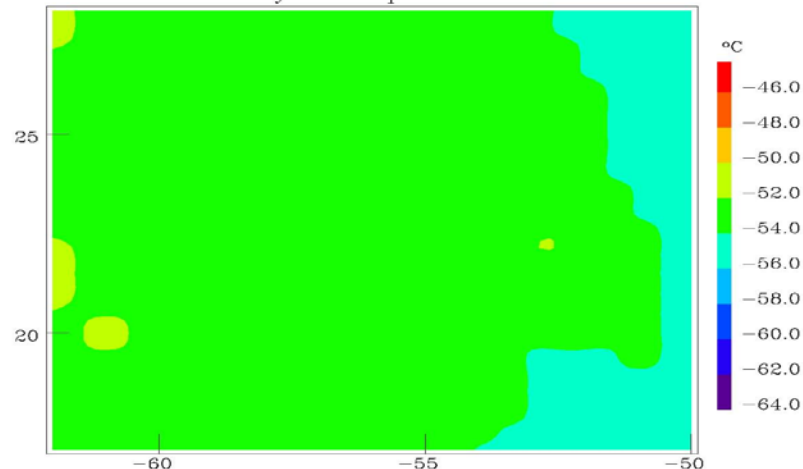
Improved 3DVAR Analysis with AMSU

Without AMSU Cloudy Radiances

GDAS Analysis Temperature at 850mb

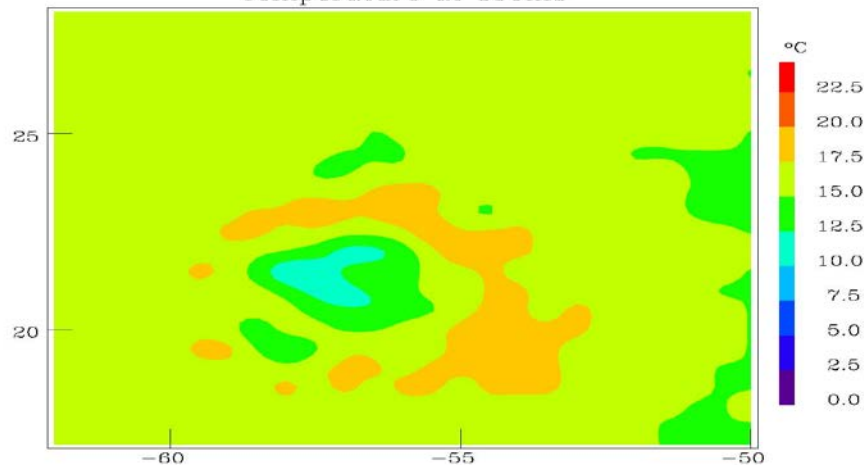


GDAS Analysis Temperature at 200mb

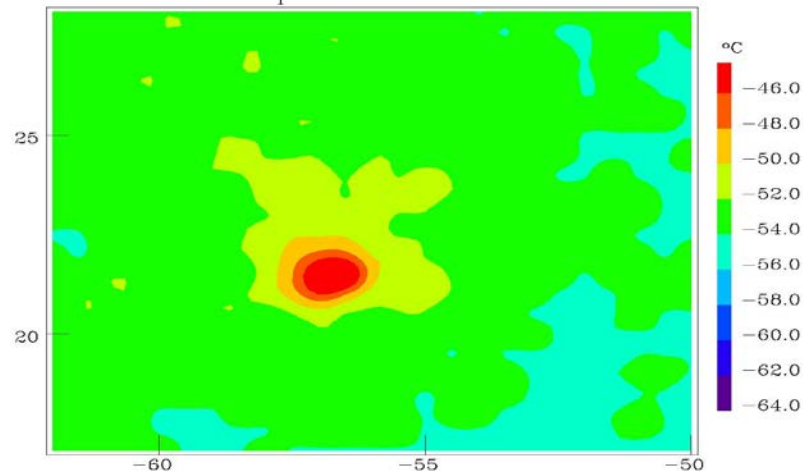


With AMSU Cloudy Radiances

Temperature at 850mb



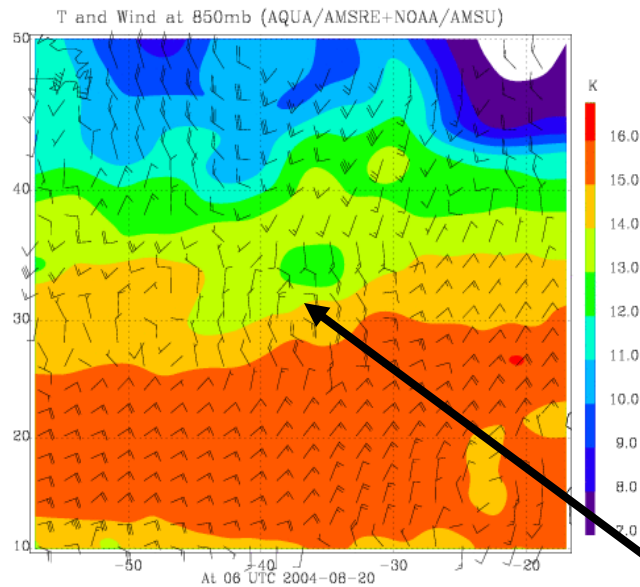
Temperature at 200mb



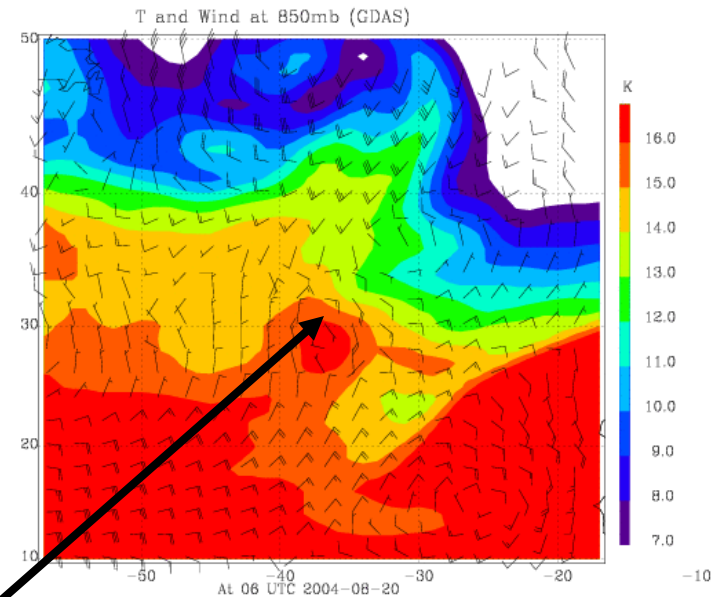
Retrievals using AMSU/AMSR-E

Hurricane Daniel

AMSU/AMSR-E



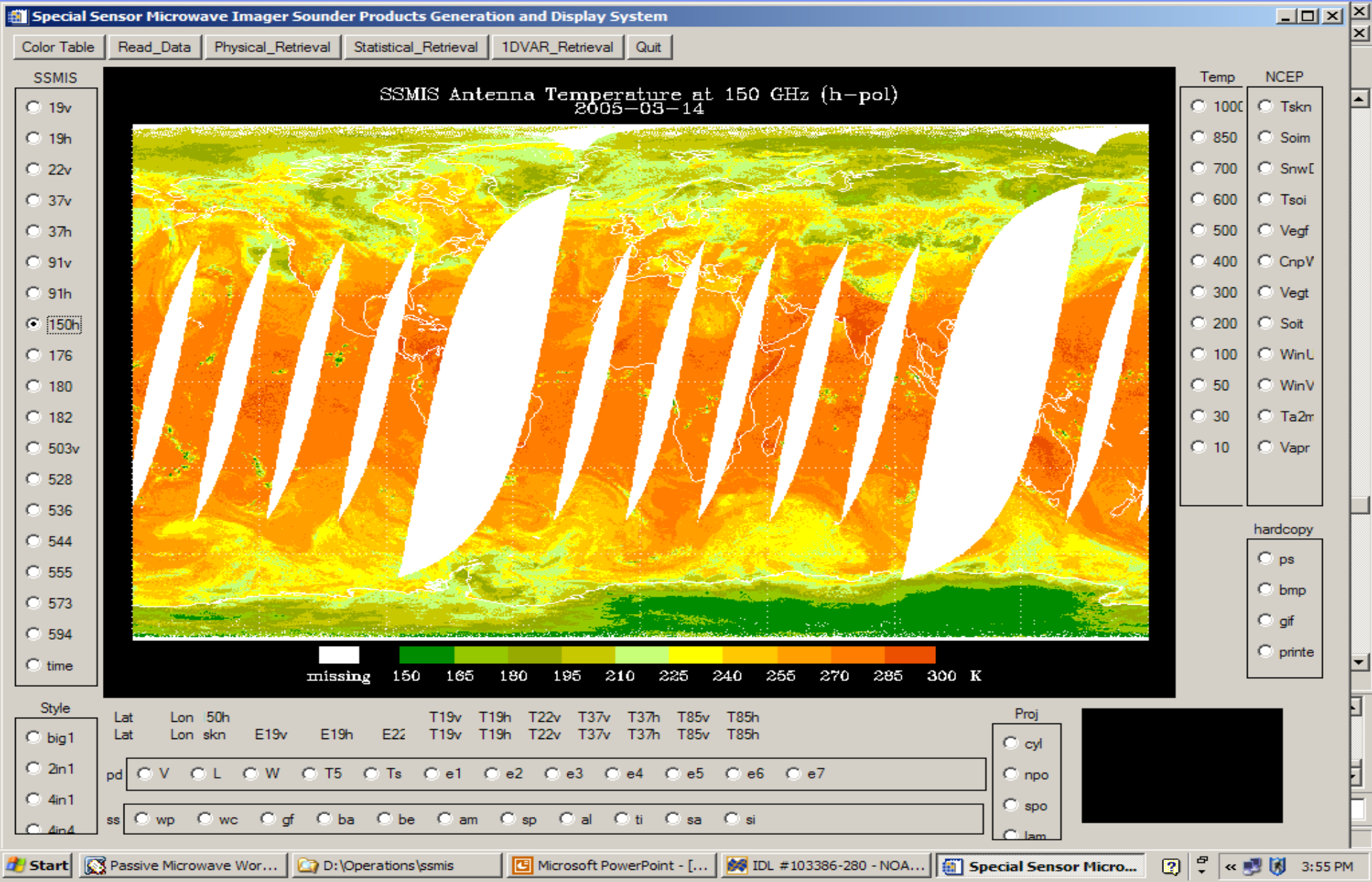
GDAS



Daniel is weakening rapidly and there is no warm core feature near center.
The analysis from NCEP/GDAS still indicates significant warming



Microwave Integrated Retrieval System (MIRS) for SSMIS





Special Sensor Microwave Imager/Sounder

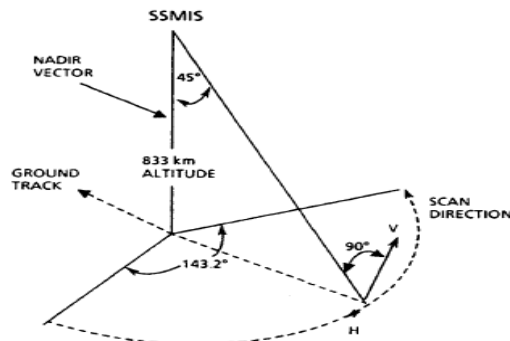
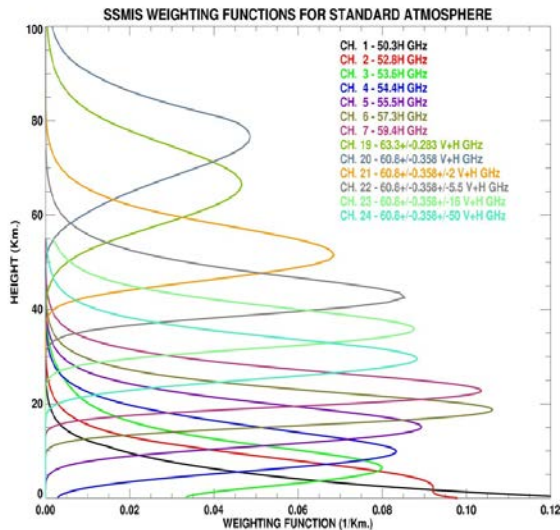


Figure 1 SSMIS Scan Geometry

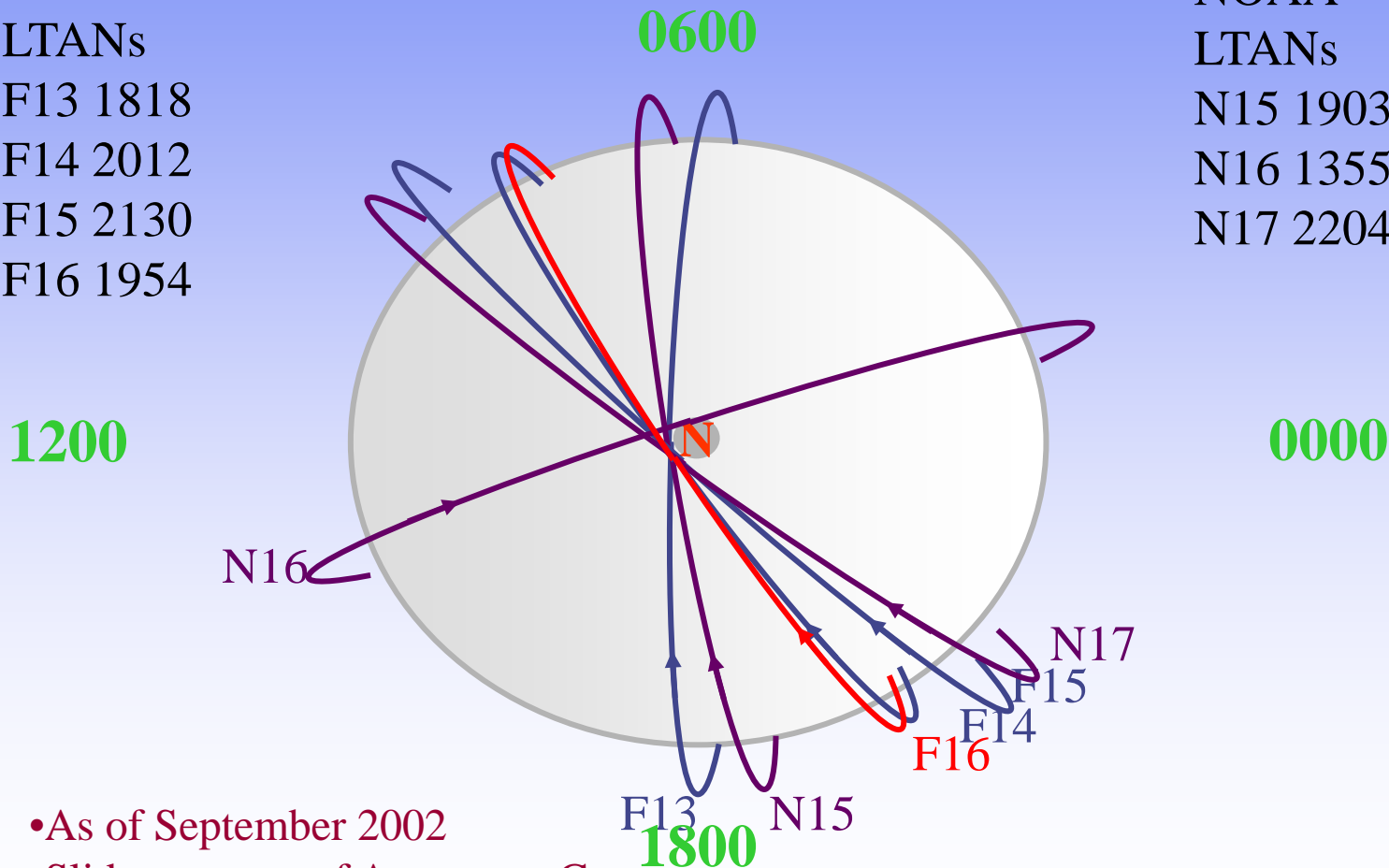
- The Defense Meteorological Satellite Program (DMSP) successfully launched the first of five Special Sensor Microwave Imager/Sounder (SSMIS) on 18 October 2003.
- SSMIS is a joint United States Air Force/Navy multi-channel passive microwave sensor
- Combines and extends the current imaging and sounding capabilities of three separate DMSP microwave sensors, SSM/T, SSM/T-2 and SSM/I.13 Channels Sfc – 80 km, compared to AMSU 13 channels (Sfc to 40 km).
- SSMIS is the first microwave sensor in space with surface imaging, temperature and humidity sounding channels combined.
 - significant potential to improve the remote sensing of the environment



Microwave Sensor Constellation

DMSP
LTANs
F13 1818
F14 2012
F15 2130
F16 1954

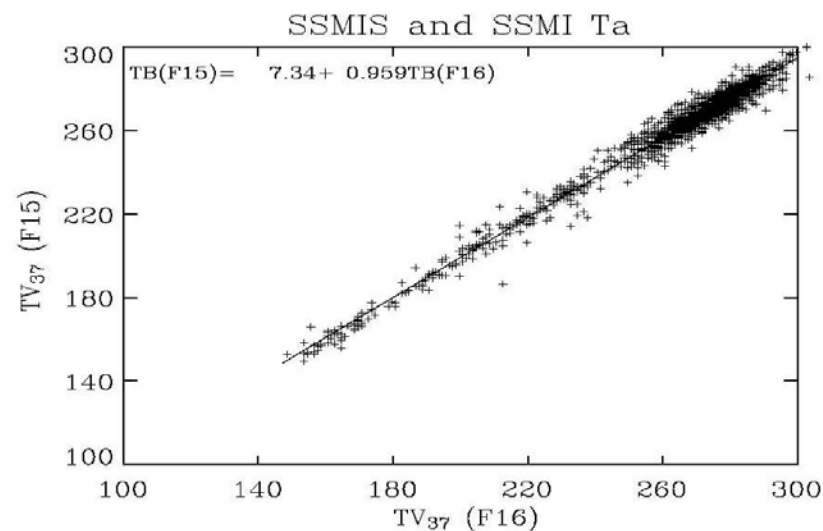
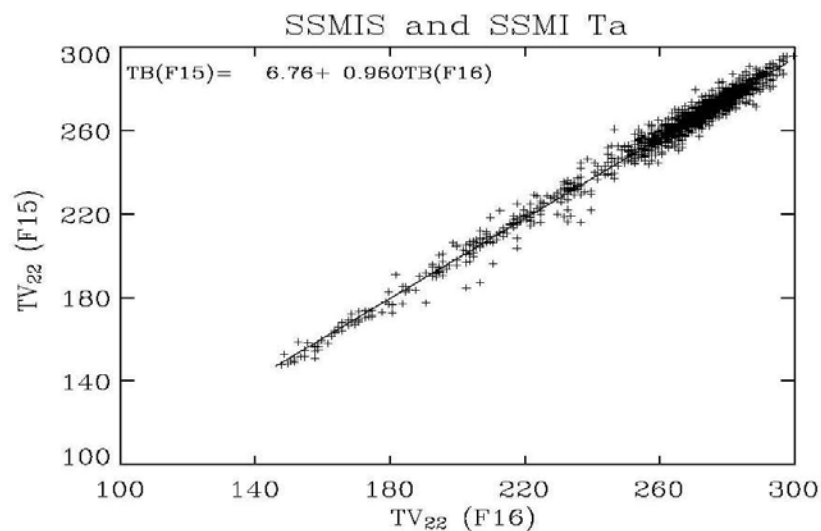
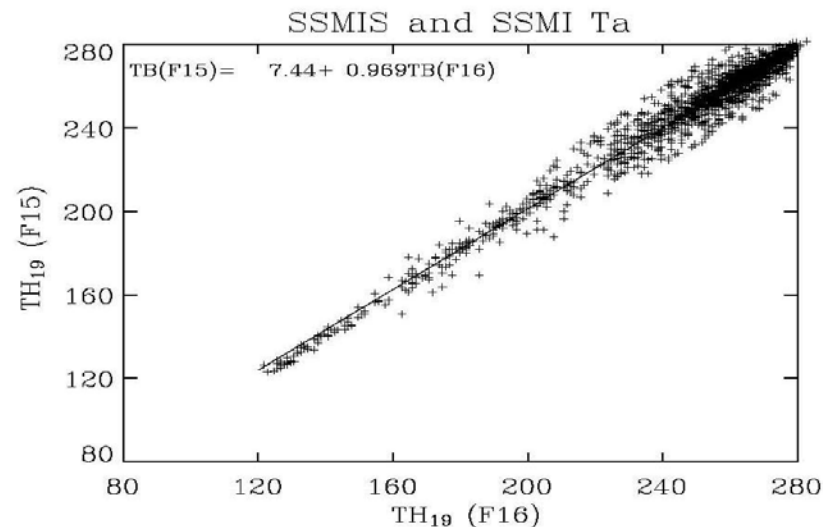
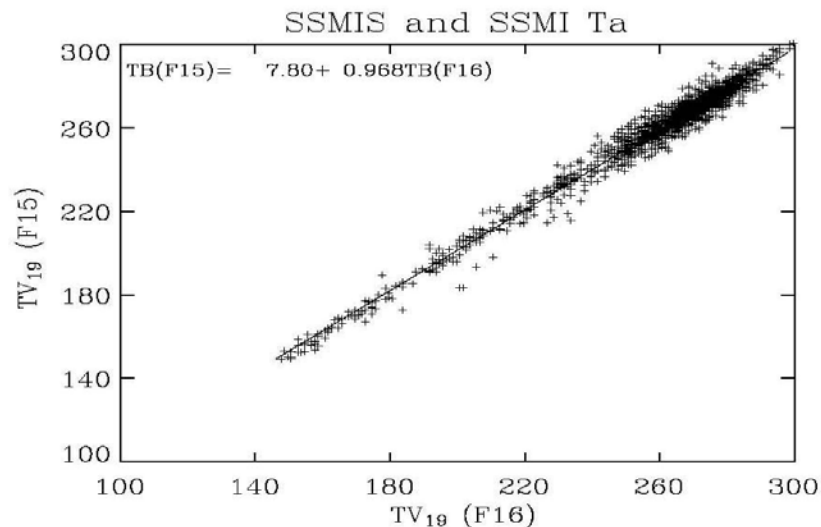
NOAA
LTANs
N15 1903
N16 1355
N17 2204



- As of September 2002
- Slide courtesy of Aerospace Corp.

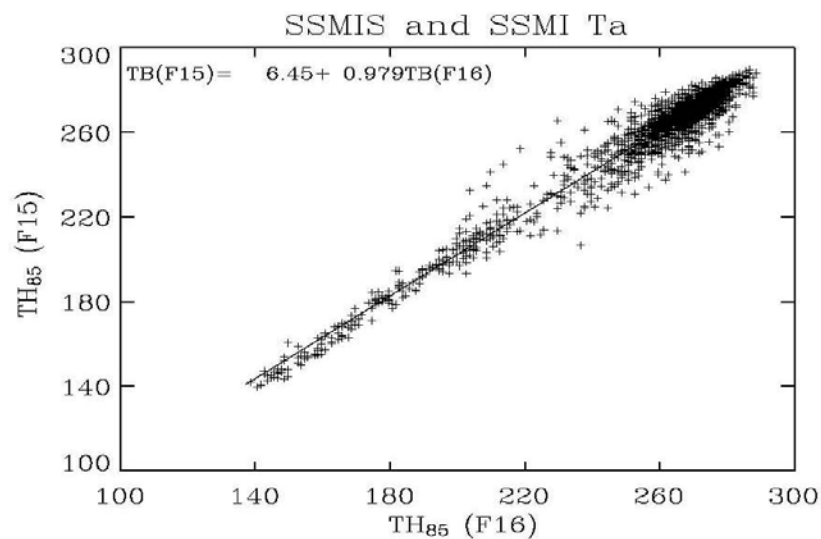
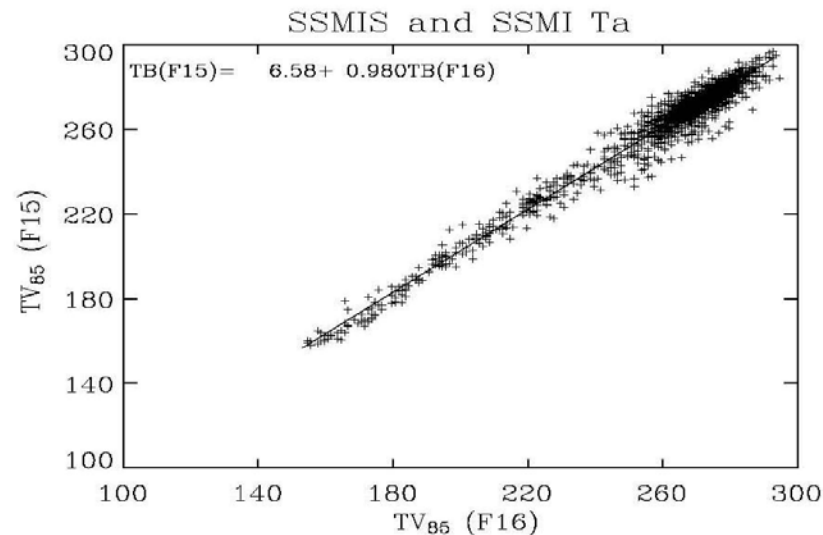
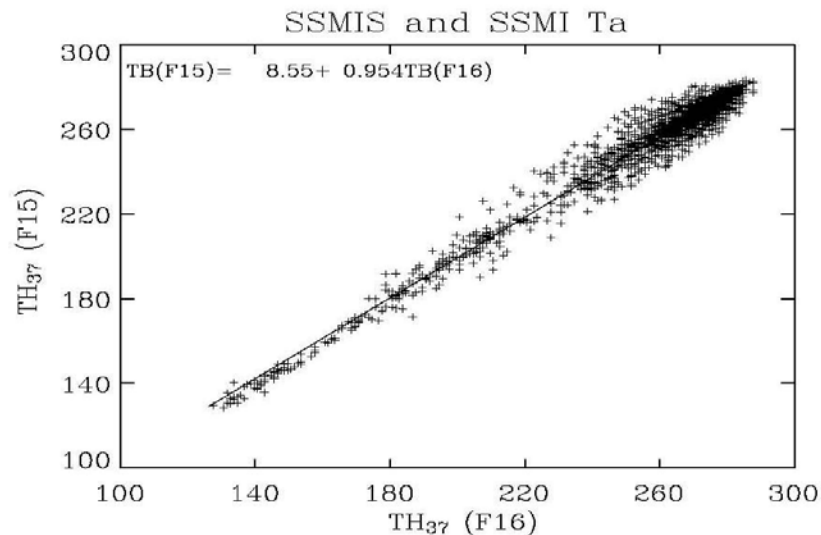


SSMIS Sensor Characterizations





SSMIS Sensor Characterizations



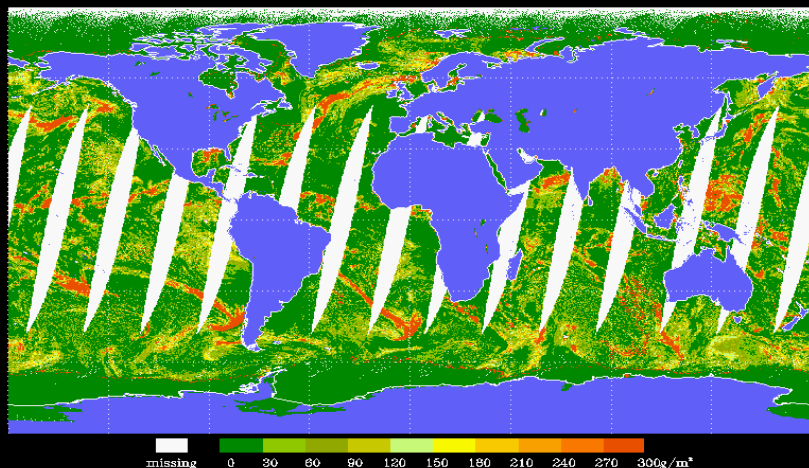


SSMIS vs. SSM/I Products

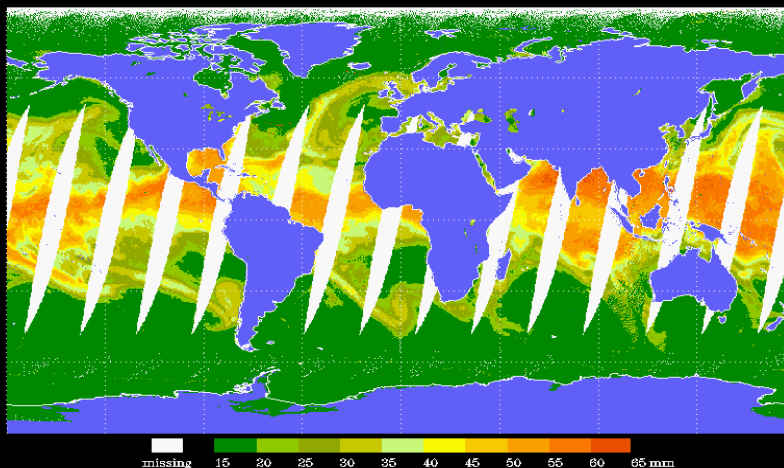
Cloud Liquid Water

Total Precipitable Water

Cloud Liquid Water Derived from SSMIS
2004-06-14

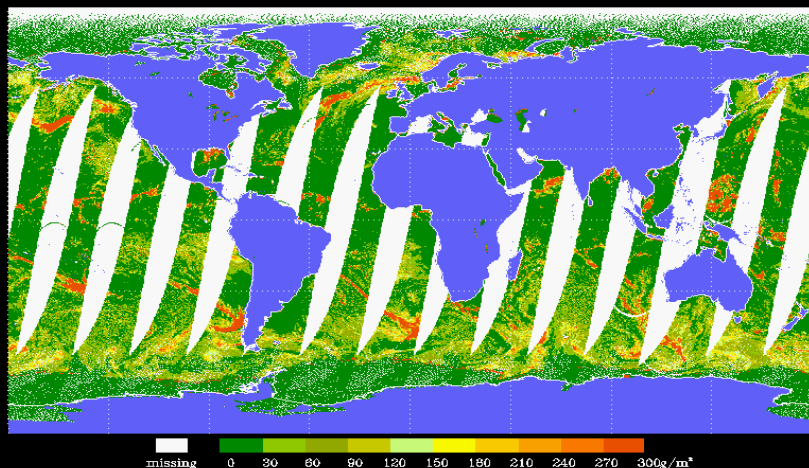


Total Precipitable Water Derived from SSMIS
2004-06-14

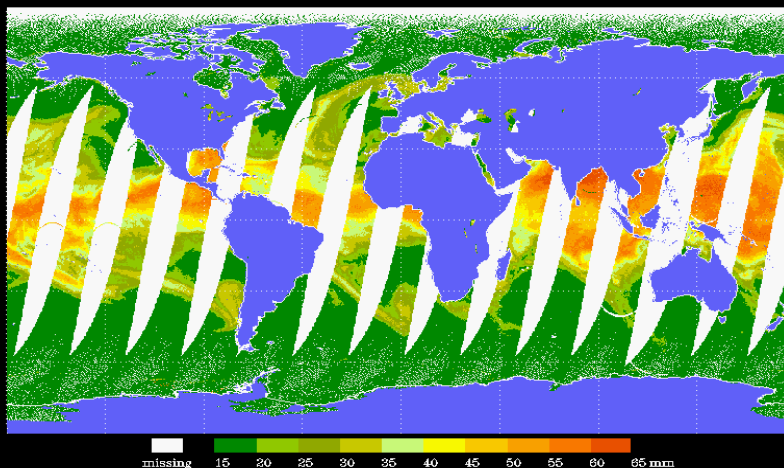


SSMIS-F16

Cloud Liquid Water Derived from SSMIS
2004-06-14



Total Precipitable Water Derived from SSMIS
2004-06-14



SSM/I-F15

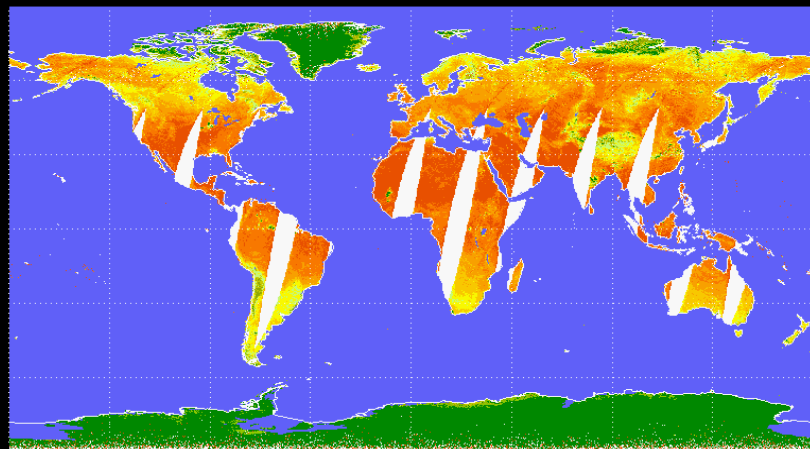


SSMIS vs. SSM/I Products

Land Surface Temperature

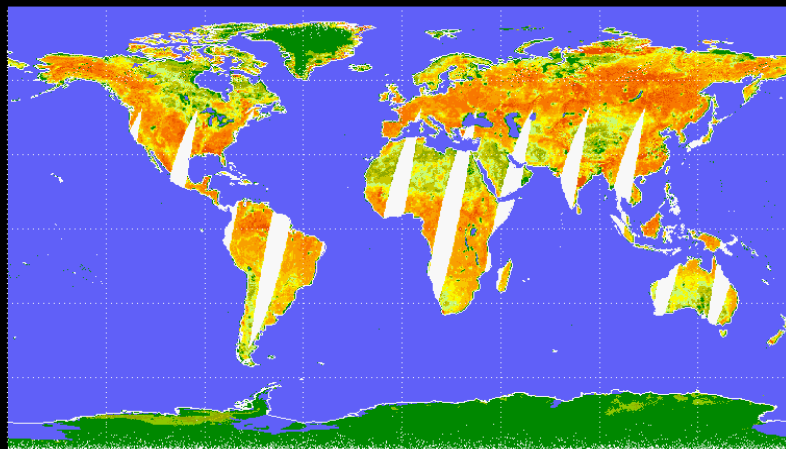
Land Surface Emissivity

Land Surface Temperature Derived from SSMIS
2004-06-14



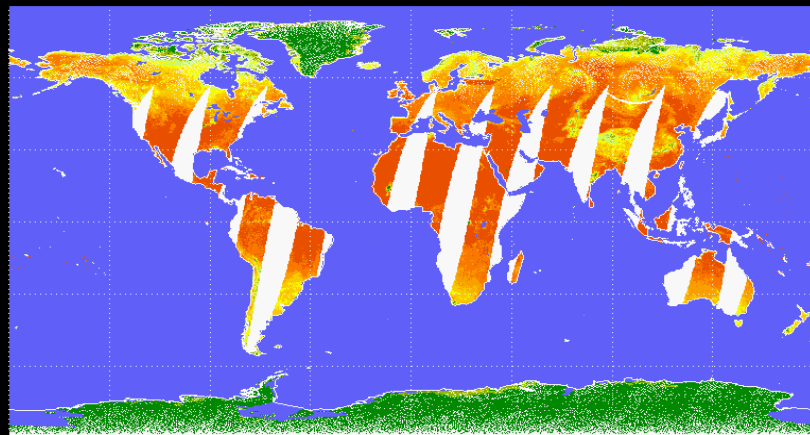
missing 250 255 260 265 270 275 280 285 290 295 300 K

SSMIS Surface Emissivity (h-pol) at 19.35 GHz
2004-06-14



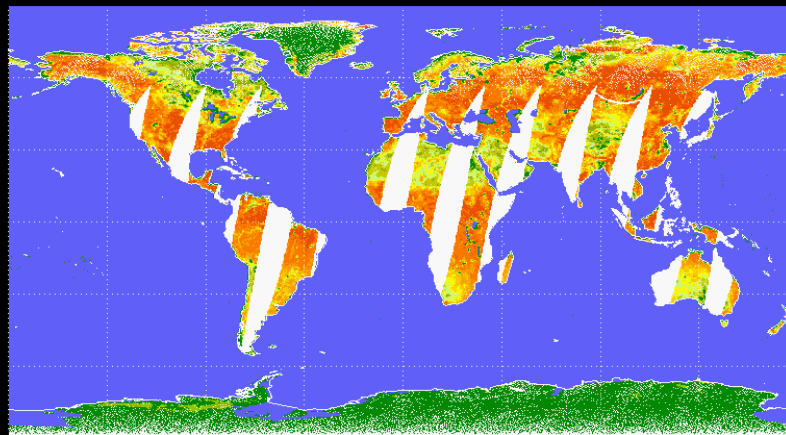
missing 80 82 84 86 88 90 92 94 96 98 100

Land Surface Temperature Derived from SSMI
2004-06-14



missing 250 255 260 265 270 275 280 285 290 295 300 K

SSMIS Surface Emissivity (h-pol) at 19.35 GHz
2004-06-14



missing 80 82 84 86 88 90 92 94 96 98 100

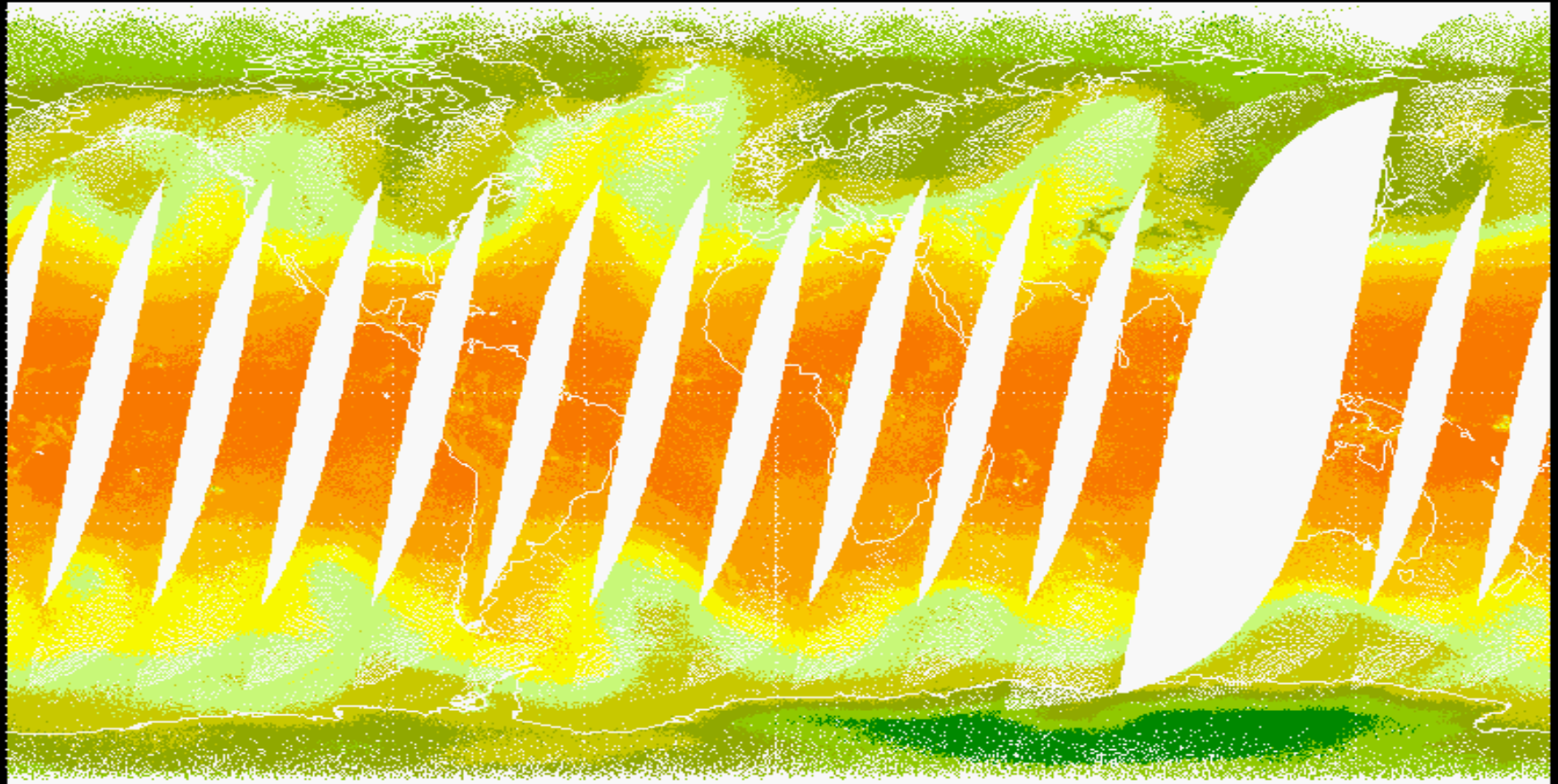
SSMIS-F16

SSM/I-F15



SSMIS Temperature at 500 hPa

Temperature at 500mb from SSMIS
2005-03-02



missing 220 226 232 238 244 250 256 262 268 274 280 K



Summary and Conclusions

- Integrated uses of microwave imager and sounder data can significantly improve temperature profiling in lower troposphere
- Advanced radiative transfer models including cloud/precipitation scattering are vital for improving profiling capability in severe weather conditions such as hurricanes
- MIRS with bias corrections to radiative transfer models produces improved performance from AMSU and makes the retrieval errors less dependent on scan angle
- MIRS retrievals are being validated against variable independent sources. Overall performances are very encouraging. The system is of great potentials for NPOESS ATMS, CMIS applications
- MIRS has a lot of room to improve and incorporate more variables in the processing.



Open Issues

- Refine the retrievals for better regional performance (e.g. high terrains, deserts, snow/sea ice cover, coast conditions)
- Bias corrections for water vapor sounding channels are highly required. Alternatively, the retrievals will be also tested with limb-adjusted AMSU measurements
- Investigate non-convergent behaviors over particular regions (scattering RT model vs. abnormal observations) in the last retrieval process when AMSU-B water vapor sounding channels are included
- Test the system for SSMIS applications